Department of Civil and Environmental Engineering

Arsenate removal from water by adsorption with magnetic nanoparticles (γ-Fe_2O_3)

Tanja Tuutijärvi

Aalto University

DOCTORAL DISSERTATIONS

Aalto University publication series
DOCTORAL DISSERTATIONS 37/2013

Arsenate removal from water by adsorption with magnetic nanoparticles (γ-Fe_2O_3)

Tanja Tuutijärvi

A doctoral dissertation completed for the degree of Doctor of Philosophy to be defended, with the permission of the Aalto University School of Engineering, at a public examination held at the lecture hall R1 of the school on 15th of March 2013 at 12 o'clock.

Aalto University
School of Engineering
Department of Civil and Environmental Engineering
Water and Environmental Engineering

Supervising professor
Prof. Riku Vahala

Preliminary examiners
Prof. Vicky L. Colvin, Rice University, The United States
Prof. Stephen J. Allen, Queen's University of Belfast, The United Kingdom

Opponent
Prof. Tuula Tuhkanen, Tampere University of Technology, Finland

Aalto University publication series
DOCTORAL DISSERTATIONS 37/2013

ISBN 978-952-60-5044-7 (printed)
ISBN 978-952-60-5045-4 (pdf)
ISSN-L 1799-4934
ISSN 1799-4934 (printed)
ISSN 1799-4942 (pdf)
http://urn.fi/URN:ISBN:978-952-60-5045-4

Unigrafia Oy
Helsinki 2013

Finland

Publication orders (printed book):
tanja.tuutijarvi@aalto.fi

Aalto University

Abstract

Aalto University, P.O. Box 11000, FI-00076 Aalto www.aalto.fi

Author
Tanja Tuutijärvi

Name of the doctoral dissertation
Arsenate removal from water by adsorption with magnetic nanoparticles (γ-Fe_2O_3)

Publisher School of Engineering

Unit Department of Civil and Environmental Engineering

Series Aalto University publication series DOCTORAL DISSERTATIONS 37/2013

Field of research Water Engineering

Manuscript submitted 12 April 2012 **Date of the defence** 15 March 2013

Permission to publish granted (date) 20 August 2012 **Language** English

☐ **Monograph** ☒ **Article dissertation (summary + original articles)**

Abstract

Arsenic is a poisonous and carcinogenic heavy metal that exists naturally on the earth's crust, from where it can leach into the groundwater – a common water source worldwide. Therefore, arsenic-rich areas pose the risk of chronic exposure, which is prevented by removing arsenic from water using various technologies. Adsorption with conventional adsorbents, as activated alumina and iron-based adsorbents, is commonly applied for arsenic removal. This study introduces a nanoscale adsorbent, maghemite-magnetic nanoadsorbent, for arsenic removal.

The overall aim of the study was to compile fundamental information on novel maghemite nanoparticles and their suitability for arsenate removal from water with laboratory-scale batch experiments. The study was conducted with three kinds of maghemites: sol-gel, mechanochemical, and commercial maghemite. Sol-gel maghemite was the main research target; the others were studied for reference. The research consisted of the preparation of maghemite nanoparticles and their characterization, the study of adsorption and desorption kinetics, an investigation of arsenate adsorption properties on maghemite, a determination of the adsorption mechanism, and an evaluation of maghemite stability and regeneration properties.

The results indicated the applicability of sol-gel maghemite for arsenate removal by adsorption. The reasons are several: Sol-gel maghemite synthesis is fast, convenient to work with and produces repeatedly high-quality particles, adsorbs arsenate satisfactorily, and there is no need for preliminary treatments prior to adsorption experiments; it is easy to handle and separate via an external magnet, it maintains its initial arsenate uptake capacity after six regeneration cycles, and it is stable, which are important factors for cost-effectiveness. And it produces only a small amount of "arsenate-maghemite" waste. Moreover, sol-gel maghemite is competitive with activated alumina in adsorbent properties. Both adsorbents need careful monitoring due to pH control, interference of other ions, and regeneration. Activated alumina can remove slightly more arsenate than sol-gel maghemite, but sol-gel maghemite is more stable, forms less waste, and is separated simply and rapidly by an external magnet.

Keywords arsenic, maghemite, magnetic nanoparticles, nanoadsorbent, adsorption, regeneration, competing ions, water treatment

ISBN (printed) 978-952-60-5044-7 **ISBN (pdf)** 978-952-60-5045-4

ISSN-L 1799-4934 **ISSN (printed)** 1799-4934 **ISSN (pdf)** 1799-4942

Location of publisher Espoo **Location of printing** Espoo **Year** 2013

Pages 136 **urn** http://urn.fi/URN:ISBN:978-952-60-5045-4

Tekijä
Tanja Tuutijärvi

Väitöskirjan nimi
Arsenaatin poistaminen vedestä adsorptiolla magneettisilla nanohiukkasilla (γ-Fe_2O_3)

Julkaisija Insinööritieteiden korkeakoulu

Yksikkö Yhdyskunta- ja ympäristötekniikan laitos

Sarja Aalto University publication series DOCTORAL DISSERTATIONS 37/2013

Tutkimusala Vesitekniikka

Käsikirjoituksen pvm 12.04.2012 **Väitöspäivä** 15.03.2013

Julkaisuluvan myöntämispäivä 20.08.2012 **Kieli** Englanti

☐ **Monografia** ☒ **Yhdistelmäväitöskirja (yhteenveto-osa + erillisartikkelit)**

Tiivistelmä

Arseeni on myrkyllinen ja karsinogeeninen raskasmetalli, jota esiintyy kallio- ja maaperässä. Sieltä arseenia voi liueta pohjaveteen, joka on yleinen juomaveden lähde maailmanlaajuisesti. Arseenipitoisilla pohjavesialueilla kroonisen altistumisen riski on merkittävä ja altistumisen estämiseksi arseenia poistetaan juomavedestä erilaisilla tekniikoilla. Adsorptio perinteisillä adsorbenteillä, kuten aktivoidulla alumiinilla ja rautapohjaisilla adsorbenteillä, on yleisesti käytössä oleva arseenin poistomenetelmä. Tässä tutkimuksessa esitetään nanomittakaavan adsorbentti - maghemiitti- magneettinen nanoadsorbentti- arseenin poistoon.

Tutkimuksen tavoitteena oli koota perustietoa uudesta maghemiittinanohiukkasesta ja sen soveltuvuudesta arsenaatin, (As(V)), poistoon vedestä laboratoriomittakaavan kokeilla. Tutkimus tehtiin kolmella erilaisella maghemiitilla, jotka erosivat toisistaan käytetyssä synteesitekniikassa: sooli-geeli, mekanokemiallinen ja kaupallinen maghemiitti, joista sooli-geelitekniikalla valmistettu maghemiitti oli päätutkimuskohde. Muut maghemiitit olivat tutkimuksessa mukana vertailutasona. Tutkimuksessa valmistettiin ja karakterisoitiin maghemiittinanohiukkasia, tutkittiin adsorptio- ja desorptiokinetiikkaa sekä arsenaatin adsorptio-ominaisuuksia maghemiittiin, määritettiin adsorptiomekanismi ja arvioitiin maghemiitin stabiiliutta ja uudelleen regeneroitavuutta.

Tulokset osoittivat sooli-geelisynteesillä valmistettujen maghemiittinanohiukkasten soveltuvan arseenin poistoon adsorptiotekniikalla. Maghemiitin syntetisointi sooli-geelitekniikalla on nopeaa, työskentely on sujuvaa ja tuloksena on toistettavasti korkealaatuisia nanohiukkasia. Sooli-geeli maghemiitti adsorboi arsenaattia hyvin eikä esikäsittelyä tarvita ennen adsorptiokokeita, sitä on helppo käsitellä ja erottaa vedestä ulkoisella magneetilla. Maghemiitilla on useita taloudellisesti ja ympäristön kannalta tärkeitä ominaisuuksia: maghemiitti säilyttää alkuperäisen arseeniin adsorptiokyvyn kuuden regeneroinnin jälkeen, on stabiili ja tuottaa vain pienen määrän arseeni-maghemiitti jätettä. Lisäksi sooli-geeli maghemiitti on kilpailukykyinen adsorptio-ominaisuuksiltaan aktivoidun alumiinin kanssa. Molempien adsorbenttien käyttö vaatii huolellista valvontaa johtuen pH:n säätötarpeesta, vedessä olevien muiden ionien häiritsevästä vaikutuksesta ja regeneroinnista. Aktivoitu alumiini pystyy poistamaan hieman enemmän arsenaattia kuin sooli-geeli maghemiitti, mutta sooli-geeli maghemiitti on puolestaan stabiilimpi, muodostaa vähemmän jätettä ja erotus vedestä tapahtuu helposti ja nopeasti ulkoisella magneetilla.

Avainsanat arseeni, maghemiitti, magneettinen nanohiukkanen, nanoadsorbentti, adsorptio, regenerointi, häiritsevät ionit, vedenpuhdistus

ISBN (painettu) 978-952-60-5044-7 **ISBN (pdf)** 978-952-60-5045-4

ISSN-L 1799-4934 **ISSN (painettu)** 1799-4934 **ISSN (pdf)** 1799-4942

Julkaisupaikka Espoo **Painopaikka** Espoo **Vuosi** 2013

Sivumäärä 136 **urn** http://urn.fi/URN:ISBN:978-952-60-5045-4

PREFACE

The research work of this thesis was carried out during the years 2007–2010 at three different universities: in 2007 at the Department of Chemical and Biomolecular Engineering at the Hong Kong University of Science and Technology (HKUST) in Hong Kong; during January–June 2008 in the Laboratory of Applied Environmental Chemistry (now the Laboratory of Green Chemistry, Lappeenranta University of Technology), Department of Environmental Sciences in the University of Kuopio in Mikkeli; and in 2009-2010 in the Water Engineering research group, Department of Civil and Environmental Engineering, Aalto University in Espoo. I gratefully acknowledge the financial support from the HKUST (HKRGC600606), the European Union, the Mikkeli University Consortium, Maa– ja vesitekniikan tuki ry, and the Aalto University School of Engineering.

I have been lucky to have three supervisors throughout this study who have dedicated themselves to their profession. I wish to express sincere gratitude to Prof. Guohua Chen for guiding me to the scientific world with his expert advice. Moreover, I appreciate Prof. Chen for taking me into his research group, thus giving me the opportunity to become familiar with the Chinese culture and work environment. I am grateful to Prof. Riku Vahala for providing me with the opportunity to finalize this study, for the motivation, and for pointing out the engineering perspective for the scientist. Last but not least, I am thankful to Prof. Mika Sillanpää for starting this project and for his enthusiasm for research.

I express my gratitude to the pre-examiners, Prof. Stephen Allen and Prof. Vicky L. Colvin, for reviewing this thesis and for their valuable comments.

I am grateful to the staff at the Water Engineering laboratory for their support and help. Special thanks to senior laboratory technician Aino Peltola and laboratory technician Marina Sushko for their assistance. I also owe thanks to the support staff at the Mikkeli laboratory. I want to thank the technicians at the Materials Characterization & Preparation Facility (MCPF), the Advanced Engineering Materials Facility (AEMF), and the Chemical Engineering Department at HKUST for their help in analysis and their incredibly fast response to questions. I especially want to thank technician Dave Ho for his assistance.

I owe great thanks to my friends for bringing humour to my scientific days and for lifting my spirits when I needed it. The warmest and loving thanks belong to my husband Mikko for his support and encouragement during these years and to our beloved sons, Ukko and Niila, for bringing joy and friskiness to my life every day.

Klaukkala, February 2013

Tanja Tuutijärvi

LIST OF PAPERS

This thesis is based on the following four papers, which are referenced in the text by the corresponding Roman numerals: I, II, III, and IV. The original papers are found in appendices I – IV.

I Tuutijärvi, T., Lu, J., Sillanpää, M., and Chen, G. (2009). As(V) adsorption on maghemite nanoparticles. *Journal of Hazardous Materials,* 166, pp. 1415-1420.

II Tuutijärvi, T., Lu, J., Sillanpää, M., and Chen, G. (2010). Adsorption mechanism of arsenate on crystal γ-Fe_2O_3 nanoparticles. *Journal of Environmental Engineering,* 136, pp. 897-905.

III Tuutijärvi, T., Vahala, R., Sillanpää, M., and Chen, G. (2012). Maghemite nanoparticles for As(V) removal: desorption characteristics and adsorbent recovery. *Environmental Technology*, 33, pp. 1927-1936.

IV Tuutijärvi, T., Repo, E., Vahala, R., Sillanpää, M., and Chen, G. (2012). Effect of competing anions on arsenate adsorption onto maghemite nanoparticles. *Chinese Journal of Chemical Engineering*, 20, pp. 505-514.

THE AUTHOR'S CONTRIBUTION

Paper I	The author carried out most of the experimental work, analyzed the data, and had the main responsibility for writing the paper.
Paper II	The author carried out all experimental work, analyzed the data, and had the main responsibility for writing the paper.
Paper III	The author carried out most of the experimental work, analyzed the data, and had the main responsibility for writing the paper.
Paper IV	The author carried out most of the experimental work, analyzed the data, and had the main responsibility for writing the paper.

ABBREVIATIONS

γ-Fe_2O_3	Maghemite
ACF	Activated carbon fiber
BET	Brunauer, Emmett and Teller method
calc	Calculated
CCD	Charge-coupled device
CNT	Carbon nanotube
EDTA	Ethylene diamine tetra-acetic acid
exp	Experimental
FA	Fulvic acid
Fe_3O_4	Magnetite
FIA	Flow injection analyzer
FTIR	Fourier transform infrared spectroscopy
HA	Humic acid
HATR	Horizontal attenuated total reflectance
HGMS	High gradient magnetic separation
ICP-MS	Inductively coupled plasma – mass spectrometry
ICP-OES	Inductively coupled plasma optical emission spectroscopy
JCPDS	Joint Committee on Powder Diffraction Standard
MIEX	Magnetic ion exchange resin
NOM	Natural organic matter
MSM	Mesostructured silica containing magnetite
nZVI	Zero-valent iron nanoparticles
POE	A point of entry
POU	A point of use
pH_{pzc}	A point of zero charge
SAMMS	Self-assembled monolayers on mesoporous supports
SSA	Specific surface area
T	Tesla
TCLP	Toxic characteristic leaching procedure
TEM	Transmission electron microscopy
US EPA	United States Environmental Protection Agency
UV-VIS	Ultraviolet-visible spectrophotometer
VSM	Vibrating sample magnetometer
WHO	World Health Organization
XPS	X-ray photoelectron spectroscopy
XRD	X-ray diffraction

CONTENTS

1. INTRODUCTION

1.1 General background

Arsenic occurs worldwide in natural water. It possesses a health risk, especially in areas where groundwater is rich in arsenic and is the main water source. Due to the toxic and carcinogenic nature of arsenic, the guideline value of arsenic in drinking water is set as low as 0.010 mg/L by the World Health Organization (WHO) [1]. The most common arsenic removal techniques are oxidation, precipitation, coagulation, flocculation, ion exchange, adsorption, and reverse osmosis [2]. Widely used and well-known adsorbents in arsenic removal are activated alumina and iron compounds. Even though they adsorb arsenic effectively, there are some drawbacks in the technique, such as high volume of sludge production and difficult separation (filtering and/or centrifugation) [3]. Forthcoming in the future are different kinds of nanomaterials with applications for arsenic removal by adsorption; these interest many researchers [4-6].

The general definition of nanoscale materials is related to their geometrical dimensions. A material is a nanomaterial when at least one dimension is < 100 nm and a second dimension is less than 1 μm [7]. Examples of nano-related materials include nanoparticles, nanotubes, nanowires, nanofibers, nanocomposites, nanoelectronics, and silicon nanostructures [8,9]. The inherent properties of nanomaterials differ from bulk material, which leads for instance to improved thermal and electrical conductivity, surface chemistry, photonic behaviour, and catalytic conversion rates [10]. Therefore, nanomaterials are of great interest in different areas, e.g., medical, pharmaceutical, environmental, electronic, and communication applications. Nanotechnology in the water sector can be utilized in the following areas: (1) treatment and remediation, (2) sensing and detecting, and (3) pollution prevention [11,12].

The use of nanomaterials in water treatment is a new and promising application. Nanotechnology-derived materials such as nanoadsorbents,

nanocatalysts, and redox-active nanoparticles, nanostructured and reactive membranes, and bioactive nanoparticles have been applied to water treatment. These materials are of interest due to their large surface area, efficiency in removing a contaminant (even at low concentrations), enhanced affinity for specific contaminant removal, catalytic potential, and high reactivity [13,14]. However, to become a reliable water treatment technique, a few challenges need to be met. So far, the environmental impact and toxicity of nanomaterials are not well known; therefore, the key challenge may be to gain regulatory and public acceptance for using nanomaterials in water purification. Other important issues to face are how to integrate nanomaterials into existing water purification systems and how to guarantee the availability of suppliers who can provide large quantities of nanomaterials at economically feasible prices [13].

In the present study, magnetic nanoparticles, maghemite (γ-Fe_2O_3), are used for arsenate removal from water. Maghemite nanoparticle as a novel adsorbent is expected to offer an attractive and inexpensive option for the removal of arsenate by considering its simple synthesizing method, large external surface area, and magnetic properties. Due to its large external surface area, it could be assumed that the adsorption capacity of maghemite nanoparticles is comparatively high and the amount of chemicals used is diminished, leading to less waste formation. Moreover, simple and rapid separation of metal-loaded magnetic adsorbent from treated water can be achieved via an external magnetic field.

1.2 Aim of the thesis

The overall aim of the thesis was to compile fundamental information of maghemite nanoparticles and its suitability for arsenate removal from water with laboratory-scale research, batch experiments. This study is fundamental due to the novelty of using maghemite nanoparticles as an arsenate adsorbent, and the results obtained in this thesis can be used in further studies.

The first objective of the study was to examine the physical properties of novel maghemite nanoparticles. In this thesis, three different kinds of maghemite nanoparticles were studied: (1) laboratory synthesized by the sol-gel process; (2) laboratory synthesized by the mechanochemical method; and (3) commercially available. Among studied maghemites, the main research interest was focused on sol-gel maghemite. Other

maghemites were studied as a reference. The second objective was to investigate the general adsorption properties of maghemites for arsenate removal. The third objective was to determine the adsorption mechanism.

1.3 Scope of the thesis

Maghemite nanoparticles were chosen for arsenate removal because of their large external surface area, their simple synthesizing method, and their magnetic properties. Moreover, they have been successfully applied for similar anion, Cr(VI), removal from water [15]. In this thesis studied three different kinds of maghemite nanoparticles were chosen according to the different particle size and synthesis method, which can have an effect on maghemite's adsorption properties.

This thesis summarizes the research reported in four papers (I-IV). The research is a fundamental study, and therefore this thesis will not give a cost estimation of nanoparticles or cover nanoparticle waste handling. However, due to the increasing interest in nanoadsorbents and to give an insight into the use of nanoadsorbents in industrial applications for arsenate removal, the literature review also consists of some information about industrially manufactured nanoadsorbents and examples of the applications.

This thesis consists of five main chapters: introduction, literature review, materials and methods, results and discussion, and conclusions. The literature review includes basic theory about arsenic and adsorption, preparation and applications of nanoparticles, and basic concepts of magnetism in magnetic nanoparticles. Moreover, it consists of sections that are more focused on practical applications in water treatment, such as magnetic separation and nanotechnology in water treatment.

In Paper I, physical properties such as particle size, particle size distribution, specific surface area (SSA), magnetization value, a point of zero charge (pH_{pzc}), and characterization of maghemite nanoparticles were presented. General adsorption properties of maghemites for arsenate removal were reported in Papers I, III, and IV. Properties studied were pH effect and isotherm (Paper I), desorption, kinetics and regeneration (Paper III), and the effect of competing ions (Paper IV). Paper II included the study of the adsorption mechanism which was conducted by macroscopic

characterization (zeta potential measurement, ionic strength effect) and microscopic characterization (FTIR, XPS, XRD, TEM).

2. LITERATURE REVIEW

A literature review consists of information in a theoretical, applied, and practical field. The theoretical background of this thesis includes basic information on arsenic and its removal, the theory of adsorption, and preparation and applications of nanoparticles, including magnetic properties of nanoparticles (sections 2.1, 2.2, and 2.4). In the applied field, magnetic nanoadsorbents for metal removal (other than arsenic) are introduced (Section 2.5.1), and nanoadsorbents for arsenate removal (both magnetic and non-magnetic) are surveyed on the laboratory scale (Section 2.5.2). Because of increasing interest in practical applications of nanoadsorbents, this thesis also includes a literature review of such applications. An overview of magnetic separation technologies in water treatment is presented due to its possible application for magnetic nanoadsorbents (Section 2.3). Industrially manufactured nanoadsorbents are introduced due to their potential for real world applications and to give an overview of the markets for nanoadsorbents (Section 2.5.2).

2.1 Arsenic

The presence of arsenic in the environment is due to natural and anthropogenic sources. It exists in the earth's crust and is mobilized by natural weathering reactions, biological activity, geochemical reactions, and volcanic emissions [3,16]. Concentrations as high as 5 mg/L of arsenic have been found in groundwater from arsenic-rich areas, and geothermal influences can increase arsenic levels, even up to 50 mg/L. Mining, smelting, and the herbicide industry are examples of anthropogenic sources of arsenic pollution [17].

Arsenic toxicity depends on its speciation, and the most significant forms for natural exposure of arsenic in drinking water are its inorganic forms [18]. Acute arsenic poisoning can cause vomiting, abdominal pain, and bloody "rice water" diarrhea [3]. Long-term exposure may lead to arsenical

skin lesions, various cancers, nausea, dryness of the mouth, and gastro-intestinal symptoms. High concentrations of arsenic in drinking water can also result in an increase in stillbirths and spontaneous abortions [18].

The occurrence of arsenic in natural waters, mainly groundwater, is a worldwide problem. Arsenic pollution has been reported in the United States, China, Chile, Bangladesh, Taiwan, Mexico, Argentina, Poland, Canada, Hungary, Finland, New Zealand, Japan, Nepal, and India [19-22]. The most alarming exposures are in Bangladesh and West Bengal in India. The guideline value of arsenic in drinking water is set as low as 0.010 mg/L by the World Health Organization (WHO) [1]. This guideline value of 0.010 mg/L has been adopted as the drinking water standard in European Union countries by the European Commission [23] and in the United States by the United States Environmental Protection Agency (US EPA) [24]. However, some countries, e.g., India, Bangladesh, Taiwan, China, and Vietnam, have retained the earlier WHO guideline value of 0.050 mg/L [25].

2.1.1 Characteristics in water

Arsenic exists in -III, 0, +III, and +V oxidation states, but in natural waters it is most commonly found in inorganic form as oxoanions: trivalent arsenite, As(III), or pentavalent arsenate, As(V). Arsenic is sensitive to mobilization at the pH values typically found in groundwater (pH 6.5-8.5) and under both oxidizing and reducing conditions [17]. Figure 2.1 shows the most important factors that control As speciation: redox potential (Eh) and pH.

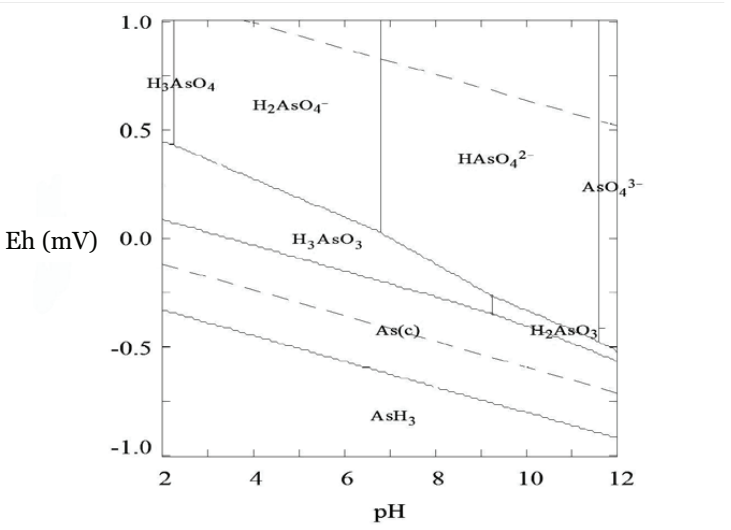

Figure 2.1. Eh-pH diagram for aqueous As species at 25°C [17].

Arsenite predominates in moderate reducing anaerobic environments such as groundwater. This is observed in Figure 2.1; uncharged arsenite H_3AsO_3 dominates under reducing conditions at pH <~9.2. In contrast, under oxidizing conditions, different dissociated forms of arsenate are dominating [26]. Speciation of arsenite (Formula 2.1) and arsenate (Formula 2.2) are expressed under differing conditions with the respective pK_a values [3].

$$H_3AsO_3 \xrightarrow[pK_a = 9.1]{} H_2AsO_3^- \xrightarrow[pK_a = 12.1]{} HAsO_3^{2-} \xrightarrow[pK_a = 13.4]{} AsO_3^{3-} \quad (2.1)$$

$$H_3AsO_4 \xrightarrow[pK_a = 2.1]{} H_2AsO_4^- \xrightarrow[pK_a = 6.7]{} HAsO_4^{2-} \xrightarrow[pK_a = 11.2]{} AsO_4^{3-} \quad (2.2)$$

2.1.2 Arsenic removal technologies

The most applied technologies for arsenic removal from water are chemical precipitation/coagulation, adsorption, ion exchange, and membrane filtration [3]. Table 2.1 provides brief descriptions of these technologies. Oxidation pre-treatment is commonly utilized before the final arsenic removal technique, since arsenite (trivalent arsenic) removal from water is more challenging than arsenate (pentavalent arsenic) [2].

The comparison among some conventional arsenic removal technologies is summarized in Table 2.2. This table indicates that the majority of low-cost methods rely on coagulation/precipitation or adsorption; ion exchange has medium costs; and membrane processes have the highest cost. The success of a particular removal technique depends on arsenic concentration to be removed, water source, competing ions (different ions in solute), waste disposal issues, population, and region where the system is located. The limitations of established techniques are production of large volume arsenic-contaminated sludge, use and handling of chemicals and its impact on water quality, possible need for secondary treatment, interference of other ions (e.g., sulphate, phosphate, silicate, iron) on removal efficiency, and high installation and operational costs [25].

Table 2.1. Descriptions of arsenic treatment technologies.

Technology	Description
Oxidation	As(III) oxidized to As(V) by chemical oxidizers, air/pure oxygen, photochemical or microbiological oxidation. Most commonly applied are chemical oxidizers such as ozone, chlorine, sodium hypochlorite, chlorine dioxide, potassium permanganate, hydrogen peroxide and Fenton's reagent [2,27,28]
Precipitation/ coagulation	Uses chemicals to transform dissolved arsenic into an insoluble solid that is precipitated (precipitation) or to adsorb arsenic onto another insoluble solid that is precipitated (coprecipitation). The solid is then removed from the liquid phase by clarification or filtration. The pH of the process highly influences the efficiency of removal. Commonly used chemicals are ferric salts, alum and manganese sulphate [25,29].
Lime softening	Precipitation where lime (lime stone, calcium hydroxide) is used for the removal [25].
Adsorption	Concentrates solutes at the surface of an adsorbent, thereby reducing their concentration in the bulk liquid phase. The adsorption media is usually packed into a column. As contaminated water is passed through the column, contaminants are adsorbed. Conventionally used adsorbents are activated alumina, activated carbon, greensand ($KMnO_4$ coated gluconite), granular ferric hydroxide, various iron compounds and copper-zinc [25,29]. The most commonly used adsorbent for arsenic removal is activated alumina [29]. Other adsorbents have also been investigated, like carbonaceous adsorbents [3] and low-cost mineral materials, e.g., dolomite [30], rice husks, chars, coals and red mud [3], and biosorbents such as chitosan [31].
Ion Exchange	Exchanges ions held electrostatically on the surface of a solid with ions of similar charge in a solution. The ion exchange media is usually packed into a column. As contaminated water is passed through the column, contaminants are removed [29].
Membrane filtration	Separates contaminants from water by passing it through semi-permeable barrier or membrane. The membrane allows some constituents to pass, while blocking others. Types of membrane filtration are microfiltration (MF), ultrafiltration (UF), nanofiltration (NF), and reverse osmosis (RO) [25].

Table 2.2. The comparison of some arsenic removal technologies [25,32,33]

Technology	Advantages	Disadvantages	Removal (%)	Relative costs
Oxidation/precipitation				
Air oxidation	Relatively simple process, in situ arsenic removal	Slow process		low
Chemical oxidation		Efficient control of the pH and oxidation step is needed		-
Coagulation/co-precipitation				
Alum coagulation	Effective over a wide range of pH; durable powder chemicals are available; simple in operation	Produces a high amount of toxic sludge; dose of oxidizing chemicals highly influence the removal efficiency	20-90	low
Iron coagulation	Common chemicals are available; proven and reliable	Produces a high amount of toxic sludge; dose of oxidizing chemicals highly influence the removal efficiency	60-90	low
Lime softening	Proven and reliable	Sulfate ions influence efficiency; sludge formation; secondary treatment is needed	80-90	low-medium
Adsorption				
Activated alumina	Relatively well known and commercially available	Careful monitoring; requires pH control; toxic solid waste due to dissolution of activated alumina	≥90	medium
Iron based adsorbents (IBS)	Plenty of possibilities, well-defined technique; no regeneration	Requires pH control; replacement of media after exhausting and regular testing to provide safe operation	≥90	low-medium
Ion exchange				
Ion exchange resin	Exclusive ion specific resin to remove arsenic; well-defined medium and capacity	Requires high-tech operation and maintenance; efficiency affected by interfering ions	≥90	medium
Membrane filtration				
Nanofiltration	Well-defined and high removal efficiency	Pre-conditioning, high water rejection, high capital cost	95	high
Reverse osmosis	No toxic solid waste is produced	High tech operation and maintenance, produces high amount of toxic reject water	≥90	high

Instead of treating arsenic in a centralized treatment system, it is possible to apply the aforementioned technologies in a smaller size for a single household, for example, in areas where each home has a private well or where centralized treatment is cost-prohibitive. Home water treatment can either be for a whole house or building (POE, point of entry) or for a single faucet (POU, point of use) [3,33].

The disposal of concentrated arsenic after water treatment raises another challenge because arsenic cannot be destroyed. It can only be converted into different forms or transformed into insoluble compounds in combination with other elements. In general, waste is treated by immobilizing the arsenic using a solidification/stabilization (S/S) technique. With this, arsenic is bound into less hazardous or non-hazardous solids (into different cements) before disposal in a landfill, thus preventing the waste from entering the environment. This technology is usually capable of meeting the arsenic leachability treatment goal (< 5.0 mg/L), as measured by the toxicity characteristic leaching procedure (TCLP) [34].

2.2 Adsorption

Adsorption is the accumulation of a substance or material at an interface between the solid surface and the solution. The adsorbate (ion or molecule in solution) is the material that accumulates at an interface of a solid surface, which is referred to as the adsorbent. Adsorption does not include surface precipitation or polymerization [35].

In adsorption, the main factors influencing the process are adsorbate and adsorbent properties as well as operational parameters of the system. Important factors in adsorbate properties are concentration, polarity, stability and configuration of the molecule, and the nature of background or competitive adsorbates. With an adsorbent, the most important determinants are equilibrium capacity (adsorption capacity) and the kinetic of equilibrium. Factors influencing previously mentioned properties are surface area, physicochemical nature of the surface [36], availability of the surface to adsorbate molecules or ions, and size and morphology of the adsorbent particles. Parameters affecting the operational system are pH, temperature, competing ions, and rate of mixing [37,38].

2.2.1 Adsorption kinetics

Prior to adsorption equilibrium studies, it is important to determine the time needed to reach the equilibrium of the process, i.e., the kinetics of adsorption. Adsorption kinetics is determined by the following stages: (1) diffusion of molecules/ions from the bulk solution towards the interface phase – so-called external diffusion, (2) diffusion of molecules/ions inside the pores – internal diffusion, (3) diffusion of molecules/ions in the surface phase (on the adsorbent surface, including the pore walls) – surface diffusion, and (4) adsorption/desorption elementary processes [39]. Generally, it can be assumed that the total rate of the kinetic process is determined by the rate of the slowest process.

2.2.2 Adsorption isotherms

Adsorption isotherm describes the adsorption equilibrium in a quantitative manner. Typically, adsorption isotherms are derived empirically by gathering data for the adsorption capacity, q_e, as a function of the adsorbate concentration in equilibrium at a certain temperature. Adsorption capacity, q_e, is calculated with the following mass balance equation (Eq. 2.1),

$$q_e = \frac{(C_i - C_e) \cdot V}{m} \tag{2.1}$$

where q_e is adsorption capacity (adsorbate per unit mass of adsorbent) in mg/g, C_i and C_e are the initial and equilibrium concentrations of adsorbate, respectively, in mg/L, V is the volume of adsorbate in litres, and m is the mass of the adsorbent in grams. Adsorption isotherms can also be derived from theoretical models for the interactions among the surface, dissolved adsorbate, and adsorbed molecules [40,41].

The behaviour of dynamic adsorption is explained by several equilibrium-based adsorption isotherm models [42]. In this study, the focus is on the simple Langmuir isotherm (one adsorbate system), which was developed by Irving Langmuir (1918). The Langmuir isotherm involves four assumptions: (1) all the adsorption sites are assumed to be identical, (2) monolayer adsorption is formed on the surface of adsorbent, (3) the adsorption energy is the same for all sites and independent of surface coverage (i.e., the surface is homogeneous), and (4) there is no lateral movement of molecules on the surface [35]. The Langmuir isotherm (Eq. 2.2) can be expressed as

$$q_e = \frac{K_{ads} \cdot C_e}{1 + K_{ads} \cdot C_e} \cdot q_{\max} \qquad (2.2)$$

where q_e is adsorption capacity (adsorbate per unit mass of adsorbent) in mg/g, C_e is the equilibrium concentration of adsorbate in mg/L, q_{max} is the maximum adsorption capacity in mg/g, and K_{ads} is a constant related to the binding strength in L/mg [35].

Adsorption in a single component system is the most often studied process. Although it does not describe the real conditions of environmental arsenic, it gives valuable fundamental information on the adsorption process. In contaminated water, environmental arsenic is always accompanied by other ions, which have an impact on the adsorption process. Because of competition of adsorption sites between ions in a multi-component system, the capacity of a single ion can be different [3].

2.2.3 Adsorption mechanism

Adsorption mechanism, or surface complexation, is the reaction between adsorbate, an ion or molecule, and the functional group of an adsorbent surface. The classification of an adsorption mechanism depends on the surface complex formed at the adsorption. Surface complexes are divided into outer- and inner-sphere surface complexes, which previously were called physical and chemical adsorption, respectively.

With outer-sphere surface complexation, the surface charge is crucial in complex formation, because electrostatic interactions and van der Waals forces (both are weak forces) are involved. The outer-sphere surface complex is separated from the inner-sphere surface complex by the existence of the water layer between the ion or molecule (adsorbate) and the surface functional group of adsorbent [35]. With inner-sphere surface complexation, a covalent or ionic bond (strong forces) is formed, and it can occur regardless of the surface charge. Formed complexes are named as monodentate and bidentate, according to the number of oxygen bonds to the adsorbed metal [35]. Figure 2.2 illustrates the surface structure of As(V) on the surface of iron oxide**.** An outer- and inner-sphere surface complex can occur simultaneously; the inner-sphere complexation is the slower process [35].

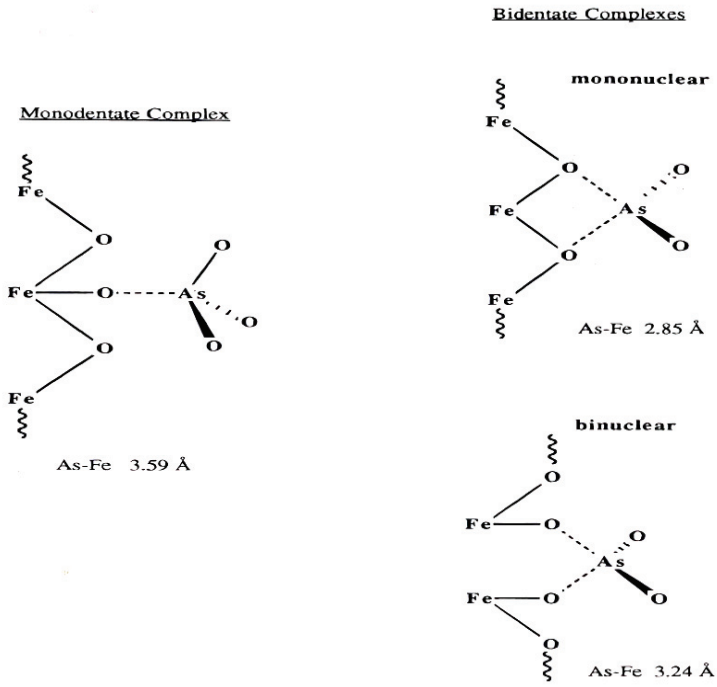

Figure 2.2. Inner-sphere complex formation of As(V) on an iron oxide surface [35].

2.2.4 The effect of competing ions

Adsorption is a removal technique whose performance is affected by other ions present in solution. This is due to several reasons, such as a limited amount of binding sites of an adsorbent (which leads to direct competition for available binding sites); alteration of a surface potential; and formation of steric effects by ions, which inhibit adsorbate adsorption onto an adsorbent surface [43,44]. Natural water consists of different ions, and in case of arsenate adsorption, the most likely competing anions are natural organic matter (NOM), phosphate, silicate, bicarbonate, nitrate, and sulphate [43]. The effect of a competing ion depends on the adsorbent, i.e., the amount of binding sites and surface chemistry, the pH of the solution, the adsorption mechanism of the anions, the relative anion concentrations, and the intrinsic binding affinities of anions [43,45,46]. Therefore, the competing effect of different anions should be studied when a new adsorbent is applied and adsorption chemical/physical conditions change remarkably.

2.2.5 Regeneration of an adsorbent

Adsorbent regeneration is a process where metals adsorbed onto adsorbent surface are recovered (desorption) and the adsorbent is regenerated. Regeneration can be either thermal or chemical. For example, the regeneration of activated carbon is conducted thermally and activated alumina chemically with alkaline/acid treatment. A successful regeneration process must restore the adsorption capacity close to its initial properties for effective use [3]. Moreover, the adsorbent should also be capable of several regeneration cycles. Desorption and adsorbent regeneration is a critical consideration and contributor to process costs and metal(s) recovery in a concentrated form. Therefore, in several treatment facilities, exhausted adsorbent is not regenerated on site but rather with an adsorbent supplier, or they may use non-regenerable adsorbents in the first place [47].

2.3 Magnetic separation technologies

2.3.1 Column and batch applications

Magnetic separation is based on the differing magnetic moments of materials, which experience different forces in the presence of magnetic field gradients. Thus, an externally applied field can separate magnetic materials (usually a solid) from a non-magnetic liquid or solid medium [48,49]. Electrically powered electromagnets or strong hard magnets can be used to separate the magnetic material [49]. Magnetic separations can be divided in column and batch applications, which are described in subsequent sections with examples.

Column applications are most likely employed in an industry where a high gradient magnetic separation (HGMS) functions as a column in continuous flow operations. An HGMS system generally consists of a column packed with a bed of magnetically susceptible wires placed inside an electromagnet. These irregular surfaces produce large magnetic field gradients that generate forces strong enough to capture even weak magnetic particles in a low stream [48,49]. The collection of particles depends strongly on the creation of these large magnetic field gradients, as well as on the particle size and magnetic properties of the material [48].

The major advantages of magnetic separation over filtration in flow systems are reasonable operating pressures and the use of conventional pumps, since the product streams meet with virtually no flow resistance as it moves

through a separator. The challenges in magnetic separation technology are related to separator design and the energy requirements of very high gradient separation [49]. Examples of industrial applications of magnetic separations are mineral post-processing [50], raw materials processing such as cement, glass, and semiconductors [51], metals production and recycling, and coal processing [49]. Recently, more complex HGMSs have been applied through the use of functionalized magnetic particles that are tailored to remove environmental contaminants such as radionuclides [52], heavy metal ions [14], and dyes [53].

In a batch system, the separation is usually conducted by a hard magnet without any external power. With appropriate magnetic material, this kind of system can remove a greater variety of substances than sedimentation can. The set-up and use of a hard magnet is easy and immediate. However, they provide relatively low magnetic gradients, which could be a challenge for the separation of small magnetic particles [49]. Batch-scale separations are most applied in biotechnological applications, for example, to purify complex mixtures for protein isolation, cell separation, drug delivery, and biocatalysis [54].

2.3.2 Water treatment and metal removal

Magnetically assisted water purification can be classified in four techniques that are based on the difference in the adoption of the physical process: (1) direct purification; (2) combination processes supported by magnetic assistance; (3) seeding and separation of magnetic flocculant, and (4) magnetic adsorbent application [55]. In the following examples of these techniques, the material removed by magnetic separation is not in nano scale. Magnetic nanomaterials will be discussed later in Section 2.5.1.

The direct purification technique utilizes the basic properties of the response of ions or solids to a magnetic field, i.e., a carrier magnetic component is not added to the process [55]. For instance, plutonium colloid has paramagnetic properties, and direct purification can be applied for its separation [56]. In combination processes, a magnetic separation has been combined in electrolytic or catalytic reactions, membrane separations, and biotechnology. Such a system has been mostly applied in landfill water purification or in environmental remediation [57].

The seeding of the magnetic component is mostly utilized in waste water treatment. During coagulation and treatment of suspended solid, oil, or

heavy metals, an iron containing magnetic powder is added to waste water. This coagulated floc containing magnetic powder can be separated by HGMS. Recently, the first full-scale HGMS device for steel mill water treatment was installed at the Chiba Plant of the Kawasaki Steel Corporation Japan [55,58]. The seeding technique has been of interest in the paper and steel industry for both oil and suspended solid removal and in the nuclear industry for radioactive sludge separation [52,59].

In case of magnetic adsorbent applications, the adsorbent can be non-functionalized or functionalized, which is also called a surface modificated, magnetic material. Examples of non-functionalized adsorbents are magnetite and maghemite. In functionalized magnetic adsorbents, functional groups are attached to magnetic substrates in order to achieve specific ion adsorption. Functional groups such silica, zeolite, polymers, and ethylene diamine tetra-acetic acid (EDTA) have shown similar features as an adsorbent alone or in junction with magnetic material, thus enabling an effective solid liquid separation [55].

Another type of magnetic adsorbent is a magnetic ion exchange resin (MIEX®) which utilizes the agglomeration property of a magnetic material. The MIEX® resin has traditional anion exchange properties combined with the magnetized iron oxide which is incorporated into the polymer matrix. The magnetic component aids the agglomeration and settling of the resin, allowing the resin beads to be smaller so that they can be applied to raw water in a slurry form [60]. Therefore MIEX® is designed to be used in a suspended manner in a completely mixed flow reactor. MIEX® is planned for the natural organic matter (NOM) removal, but it is capable of removing some inorganic ions such as As(V) and Cr(VI) [61].

2.4 Nanoparticles

Nanoparticles are defined as particles that are less than 100 nm in size. They can be spherical, tubular, or irregularly shaped and can exist in infused, aggregated, or agglomerated forms. The source of nanoparticles can be natural (e.g., volcanic activities and wild fires) or of anthropogenic origin, such as engineered nanoparticles or combustion by-products [62]. Nanoparticles can be divided into carbon-containing and inorganic nanoparticles. Most interest in carbon-containing nanoparticles is focused on fullerens, carbon nanotubes, and polymeric nanoparticles. Inorganic nanoparticles are different oxides and metals (e.g., nanowires and quantum

dots), clays, aerosols (sea salt), aluminosilicates (zeolites, ceramics), and combustion by-products (platinum group metals) [8,62].

Nanoparticles are of great interest because of their novel physicochemical properties, high chemical and biological reactivity, and capability of precise design for specific purposes, especially in the case of engineered nanoparticles [62]. The reason for the change in nanoparticles' physicochemical properties compared to bulk material is their small size and increased surface area. As the particle size decreases, a large percentage of all the atoms or molecules are located on the surface of the particles, while in conventional materials they are located in the bulk [9]. Thus the properties of the nanoparticles are more closely related to the states of individual molecules, molecules on surfaces or interfaces than to the properties of the bulk material, and these phenomena change the properties of nanoparticles [7].

2.4.1 Preparation of nanoparticles

Nanoparticle preparation can be classified several ways, from which physical and chemical synthesis methods are applied here. In the physical synthesis method, generation of nanoparticles includes high-energy treatment of the gaseous or solid material, while in the chemical synthesis method, the nanoparticle synthesis is often carried out in solutions at moderate temperatures [63].

Physical synthesis methods

In the condensation (deposition) method, molecules and atoms are transformed into a gas phase by heat and usually under vacuum. Then vaporized/ionized material is condensed to a deposited form, either as nanocrystals or surface coating [9]. Material evaporation can be induced by laser, thermal, plasma (arc discharge), and solar energy induced vaporization as well as by chemical vapour condensation (CVC) and electrodeposition [7,64-67].

The mechanochemical method involves a mechanical activation (crushing) of solid-state displacement reactions by the milling of precursor powders, which form nanomaterials. The formed nanocrystalline particles are dispersed within a soluble salt matrix, which selective removal by an appropriate solvent(s) yields nanoparticles of the desired phase [68,69]. Chemical reactions occur at the interfaces of the nanometer-sized grains that are continuously regenerated during milling. This nanometer-size grain enhances the reaction kinetics, enabling chemical reactions that

otherwise would only occur in a high temperature during milling [9]. The mechanochemical method is capable of producing nanoparticles with small particle sizes, low agglomeration, narrow size distributions, low cost, and uniform crystal structure and morphology [69]. The major disadvantages in this method are time-consuming synthesis (several hours to several days) and product contamination during the milling process [67].

Chemical synthesis methods

The following methods are all classified as chemical synthesis methods of nanoparticles: (1) co-precipitation, (2) thermal decomposition (3) sonochemical, (4) microemulsion, (5) hydrothermal, and (6) sol-gel methods [67,70-72]. Table 2.3 describes the principles of different chemical synthesis methods. Particle size distribution is generally found to be narrow in chemical methods, and the yield of nanoparticles is high, except with microemulsion and sonochemical methods. The disadvantages of chemical synthesis method are high cost and use of solvent in some methods. In terms of synthesis simplicity, co-precipitation and sol-gel are the preferred routes [67,70,71].

Table 2.3. Chemical methods for nanoparticle synthesis.

Synthesis method	**Principle of synthesis**
Precipitation/ Co-precipitation	The products of precipitation reactions are generally low soluble species formed under high supersaturation conditions. Precipitation is commonly induced by chemical reaction, e.g., addition/exchange, reduction, oxidation, photoreduction and hydrolysis [70].
Thermal Decomposition	A chemical reaction in which a chemical substance breaks down into at least two chemical substances when heated [71].
Sonochemical	Molecules undergo a chemical reaction due to an application of powerful ultrasound radiation [72].
Microemulsion	Water/oil microemulsion solutions are nano-sized water droplets dispersed in the continuous oil phase and stabilized by surfactant molecules. These surfactant-covered water pools offer a unique microenvironment for the formation of nanoparticles [67].
Hydrothermal	Polar or nonpolar solutions, vapours, and/or fluids react with solid materials at high temperature and pressure. If the solvent used is nonpolar, synthesis is called solvothermal synthesis [67].
Sol-gel	Based on a polymerization reaction, which is possible in both organic and inorganic routes. It includes four steps: hydrolysis, polymerization, growth, and gelling [9].

A more detailed analysis of sol-gel synthesis will be given here, since it is the main synthesis method applied in this thesis for maghemite preparation. Sol-gel synthesis is possible in both organic and inorganic routes. With the organic route (alkoxide route), the starting material

typically employed is metal alkoxide in organic solvent. The applied metal and alkoxy group (i.e., different functional groups) in synthesis depends on the product of interest, whereas the inorganic route (colloidal route) uses metal salts in an aqueous solution (chloride, oxychloride nitrate) as raw materials [73].

General sol-gel formation for both organic and inorganic precursors occurs in four stages: (1) hydrolysis, (2) polymerization and/or condensation, (3) growth, and (4) agglomeration of particles i.e., gelling [9]. Sol (colloidal suspension) is formed during hydrolysis and polymerization/condensation reactions after the mixing of reactants, typically with a catalyst (acid or base). The resulting solid particles are so small that gravitational forces are insignificant and interactions are dominated by van der Waals, coulombic, and steric forces. These sols are stabilized by an electric double layer, or steric repulsion, or a combination of both. Over time, the colloidal particles link together (growth of particles) and form a dimensional network that extends throughout the liquid (gelling) [73].

The size of the sol particles depends on the solution composition, pH, and temperature. When these factors are controlled, it is possible to tune the size of the particles. Also varied nanoproducts such as films/coatings, aerogels, ceramics, and fibers are possible to form with different post-treatments (evaporation, extraction, heating) of sol or sol-gels [74-78]. One synthesis derivation is precipitation, which is commonly used for uniform nanoparticle production. Sol-gel methods are most commonly used to synthesize oxides, although the synthesis of carbides, nitrides, and sulfides by sol-gel processes were also reported [70].

2.4.2 The magnetic properties of nanoparticles

The origin of magnetism lies in the orbital and spin motions of electrons and how the electrons interact with one another. The magnetic behaviour of particles can be classified into five major groups: dia-, para-, ferro-, ferri-, and antiferromagnetism [79]. Moreover, another form of magnetism, superparamagnetism, is known to exist for small nanoparticles [80].

Diamagnetic material does not possess any magnetic behaviour internally or when a magnetic field is applied on it. Paramagnetic material can be magnetized by an external magnetic field, but its magnetization is zero when the magnetic field is removed [79]. Ferromagnetic material is easily magnetized, and it can be divided into two subclasses: hard and soft magnets. Hard magnets remain magnetized after the field is removed, while

soft magnets do not [81,82]. Antiferromagnet is a “so-called” subclass of ferromagnet, and it does not remain magnetized as a hard magnet after it is removed from the magnetic field [81,82].

In ionic compounds, such as oxides, more complex forms of magnetic ordering can occur as a result of the crystal structure. This kind of magnetic ordering is called ferrimagnetism and it is similar to ferromagnetism [79]. Superparamagnetism is a form of magnetism that appears in small ferromagnetic or ferrimagnetic nanoparticles [80]. Superparamagnetism occurs in nanoparticles that are single-domain, i.e., composed of a single magnetic domain. This is possible when their diameter is less than 3 to 50 nm. The relation of superparamagnetism to particle diameter depends on the material of the nanoparticle [81].

Figure 2.3 shows theoretical magnetization curves possible to obtain by vibrating sample magnetometry (VSM), which is one of the important techniques to measure the sample’s net magnetization. Graph 2.3.a shows the characteristic magnetization curve of a ferromagnetic material – high remanence magnetization (M_r) and high coercivity (H_c). Remanence magnetization (M_r) implies that material has magnetization remaining after an external magnetic field is removed. Coercivity (H_c) is the intensity of the applied magnetic field required to reduce the magnetization of that material to zero after the magnetization of the sample has been driven to saturation.

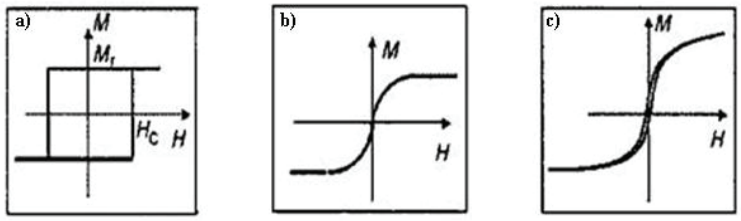

Figure 2.3. The different magnetic effects occurring in magnetic nanoparticles: (a) hard ferromagnetic material; (b) superparamagnetic material; (c) weak ferromagnetic material (modified from [81]).

Graph 2.3.b shows a typical magnetization curve of a superparamagnetic material. Hysteresis does not occur in this magnetization curve because the remanence and coercivity are both zero. Superparamagnetic material behaves in manner similar to paramagnetic material [81]. Weak ferromagnetic material has a slight hysteresis in the magnetization curve due to the existence of low remanence and coercivity (Graph 2.3.c).

Superparamagnetic and weak ferromagnetic materials are examples of soft magnets [55].

Two key issues known to affect the magnetic properties of nanoparticles are particle size and surface effects such as different kinds of coatings. The magnetic behaviour of nanoparticles is a result of both the intrinsic properties of the particles and the interactions among them. The distribution of the sizes, shapes, surface defects, and phase purity are only a few of the parameters influencing the magnetic properties, which makes the investigation of the magnetism in small particles very complicated [81].

2.4.3 Applications of nanoparticles

The use of nanoparticles is widely reported in a variety of areas such as electronic, magnetic and optoelectronic, biomedical, biological, pharmaceutical, cosmetic, energy, environment/environmental detection and monitoring, catalytic, and advanced materials applications. Nanoparticles are used in semiconductor chips, ceramics, coatings, paints, sunscreens, plastics, fillers, and tips for scanning probe microscopes [8,10,83]. Promising medical applications encompass diagnostic and drug delivery systems [84,85]. Moreover, there exist several kinds of nanoparticle applications that focus on pollution prevention and treatment (e.g., different kinds of pollutant sensors, destruction of bacteria), and removal of environmental contaminants from various media with different kinds of methods (e.g., water treatment, post-treatment of contaminated soil, sediments and solid wastes) [86-89]. There are also diverse applications existing for magnetic particles, as in recording tapes, catalysts, and in biotechnology/biomedicine applications [90,91].

2.5 Nanotechnology in water treatment

Nanotechnology offers the potential to use novel nanomaterials for water treatment to provide efficient, cost-effective and environmentally acceptable solutions to improve water quality and to increase quantities of potable water. The nanotechnology applications employed in water treatment is summarized in Figure 2.4. Membrane processes are the most versatile techniques in pollutant removal, since they are capable of removing inorganic, organic, and biological contaminants (i.e., bacteria and viruses) as well as radionuclides [92,93]. Moreover, nanofiltration alone or combined with reverse osmosis has been applied to desalination [93,94].

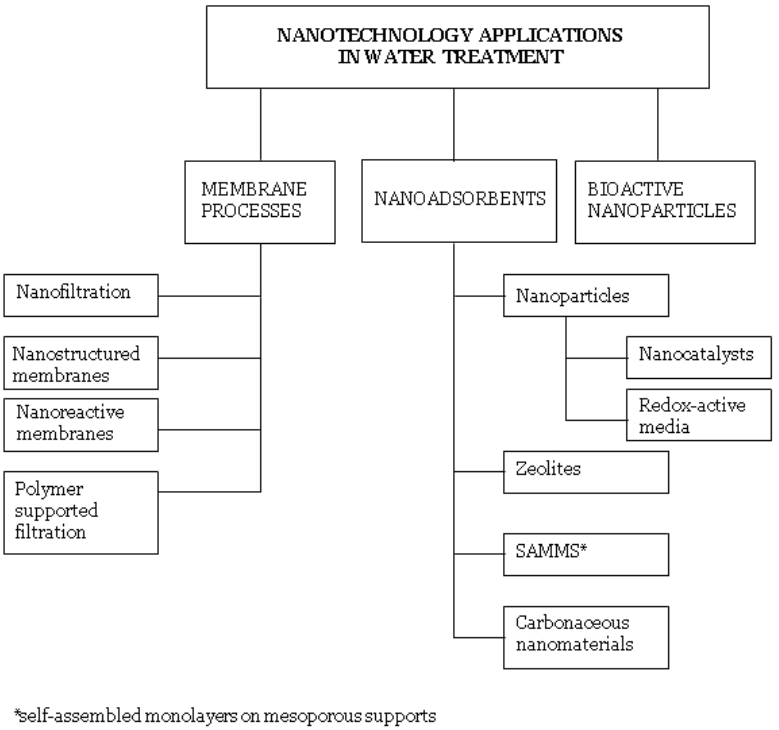

Figure 2.4. Nanotechnology applications in water treatment [13].

An emerging technology in water treatment is the use of nanoadsorbents for heavy metals, organic pollutants, and radionuclides removal. This is because nanoadsorbents have a large surface area, the number of surface atoms is numerous enabling novel reactions at the nanoscale, and they can also be functionalized with various chemical groups or have their surface modified to increase their affinity towards target compounds [13,14]. Furthermore, less waste is generated by nanoadsorbents since less adsorbent is required because more adsorbent atoms are present per unit mass of the adsorbent as with bulk adsorbents [14]. Another advantage among magnetic nanoparticles is that separation of the adsorbent from water can be conducted by a magnetic field, which makes the separation process fast and convenient.

Frequently studied nanoparticles in water treatment are iron and aluminium oxides, either plain or functionalized ones [14]. Interest in magnetic nanoparticles is also increasing, since the possibility to remove a used adsorbent with a magnet is an immense benefit compared to non-magnetic adsorbents [6,15,95]. A special group among nanoparticles consists of titanium oxide (TiO_2) and zero-valent iron (nZVI), which can be used as a “plain” adsorbent or either as a catalyst (TiO_2) or redox-active

media (nZVI) [89,96,97]. Zeolites are effective adsorbents and ion-exchange media for metal ions. They are inorganic crystalline porous materials, which have a highly ordered structure and are generally comprised of silicon, aluminium, and oxygen. Self-assembled monolayers on mesoporous supports (SAMMS) is a new class of environmental adsorbent materials; the simplest can be described as functionalized nanoporous ceramics [13]. It can effectively remove metal ions, anions, and radionuclides. Activated carbon fibers (ACFs), carbon nanotubes (CNTs), and fullerenes are the main carbonaceous nanomaterials employed as adsorbents. They have high capacity and selectivity for organic solutes in aqueous solutions [98-100].

Bioactive nanoparticles are suitable for water disinfection, and they may present an unprecedented opportunity to develop chlorine-free biocides. Among the most promising nanomaterials with antimicrobial properties are metallic and metal-oxide nanoparticles (e.g., silver and silver compounds, magnesium oxide) as well as titanium oxide photocatalysts [96,101,102].

2.5.1 Magnetic nanoadsorbents

Scaling down the size of a magnetic adsorbent to nanosize has introduced new adsorbent family, magnetic nanoadsorbents, to the water treatment sector. However, in the case of magnetic materials, scaling down may disclose undesired characteristics in a magnetic material compared to a bulk one. For example, downsizing can form hard magnetic material, which could make magnetic filter regeneration difficult [55]. Therefore the preferred magnetic nanoadsorbents for magnetic separation applications are soft magnets with low magnetic remanence (weak ferromagnetic material) and zero magnetic remanence (superparamagnetic material) [55].

Since magnetic nanoadsorbents have not been widely used for As(V) removal, other metals removed by them are discussed here more detail to show examples of magnetic nanoadsorbents' modifications and performances. Recently, magnetic nanoadsorbents have been employed for Co(II), Cu(II), Ni (II), and Cr(VI) removal [15,103-111]. In all of these studies, an adsorbent was separated by a magnet from the solution. Functionalized magnetic nanoadsorbents was applied for Co (II) and Ni (II) removal. Cu(II) and Cr(VI) removal was tested both with non-modified maghemite and a surface modified one. As(V) removal from water with non-magnetic and magnetic nanoadsorbents will be discussed in Section 2.5.2.

Co(II) and Ni(II) removal

Co(II) adsorption onto magnetic chitosan nanoparticles was studied with particles of 13.5 nm in size. Preparation of chitosan nanoparticles was conducted in two steps. First, chitosan was synthesized by carboxymethylation and then it was bound onto the surface of magnetite (Fe_3O_4) nanoparticles via carbodi-imide activation. The particles' magnetic properties were nearly superparamagnetic, with a saturation magnetization of 62 emu/g. The maximum adsorption capacity of Co(II) was 27.4 mg/g at pH 5.5 with an adsorbent dose of 21 g/L and an initial cobalt concentration of 1500 mg/L [111].

Ni(II) removal was applied by using magnetic alginate microcapsules containing the extractant Cyanex 272. The magnetic material used was maghemite, which was coated with citrate anions to enable the reaction with sodium alginate polymer. The alginate polymer was formed by mixing sodium alginate and sodium azide. Cyanex 272 was added to the maghemite and alginate polymer mixture. Finally, water-insoluble calcium-alginate microcapsules were formed by adding $CaCl_2$ into viscous water-soluble sodium alginate. The adsorption capacity of Ni was 30.5 mg/g at pH 5.3 with a adsorbent dose of 7.2 g/L with a varying nickel concentration. The magnetic separation was conducted by using ~1 Tesla magnetic field [110].

Cu(II) and Cr(VI) removal

Non-modified and gum-arabic modified magnetite [103] and mesostructured silica containing magnetite (MSM) [109] were utilized for Cu(II) removal. The interaction of gum arabic carboxylic groups and the surface hydroxyl groups of magnetite generate modified magnetic nanoadsorbent where the amine groups of gum arabic form complex with copper. The adsorption capacity of Cu(II) with gum arabic modified magnetite was twofold, 38.5 mg/g, compared to plain magnetite. Experiments were conducted at pH 5.1 with an adsorbent dose of 5 g/L and initial copper concentration of 200 mg/L [103]. The Cu(II) adsorption capacity with MSM was 31.8 mg/g with an adsorbent dose of 5 g/L at pH 4 with the initial copper concentration range of 0-1300 mg/L. MSM was synthesized by the electrostatic interaction between large magnetite particles (mainly 100 nm) and nanostructured silica (3 nm of pore diameter). Here, as in gum arabic modification, formed amine onto the magnetite surface acted as a functional group for copper removal [109].

The use of magnetic nanoparticles in wastewater treatment has been investigated in the recent past. These studies have focused on heavy metal,

mainly Cr(VI), removal by magnetite [104], maghemite [15,106], and surface modified magnetic nanoparticles [105,107,108]. Magnetite (Fe_3O_4) was effective for the removal of Cr(VI) from wastewater, but due to chemical adsorption in the process, the regeneration of adsorbent and recovery of adsorbate became difficult and inefficient [104]. Adsorption of Cr(VI), Cu(II) and Ni(II) onto maghemite followed the Langmuir isotherm model. Adsorption capacities were 17.4 mg/g Cr(VI), 27.7 mg/g Cu(II) and 25.7 mg/g Ni(II). Regeneration studies indicated that maghemite nanoparticles undergoing successive adsorption-desorption processes retained the original metal removal capacity [106]. The effect of coexisting ions (Na^+, Cu^{2+}, Ni^{2+}, Ca^{2+}, Mg^{2+}, NO_3^-, and Cl^-) on Cr(VI) removal by maghemite was found to be insignificant, which illustrated the selective adsorption of Cr(VI) from wastewater [15]. Surface modified magnetic nanoparticles studied for Cr(VI) removal were δ-FeOOH (inorganic feroxyhyte)-coated maghemite and six different kinds of ferrites, $MeFe_2O_4$ (Me= Mn, Co, Cu, Mg, Zn, Ni). The adsorption capacity of the δ-FeOOH-coated maghemite was 25.8 mg/g; and the highest adsorption efficiency, 99.5%, was found for $MnFe_2O_4$ nanoparticles [105,107,108].

2.5.2 Nanoadsorbents in arsenic removal

Presently the applications of nanoadsorbents are developing as an area of interest for arsenate removal from water. Several studies have been conducted to investigate the suitability of different nanoadsorbents to remove arsenate from water (Table 2.4). Moreover, a few industrially manufactured nanoadsorbents are already on the market to treat arsenate containing water at least POU-level (Table 2.5). However, it should be kept in mind that the use of nanoadsorbents in industrial applications is not routine at the moment. The breakthrough of nanoadsorbents in practical applications is affecting their potential environmental and human health risks, i.e., a lack of coherent information on their behaviour, which also generates socio-economic issues [112].

Laboratory scale applications of non-magnetic nanoadsorbents

Table 2.4 shows different nanoadsorbents and optimum operating conditions for arsenate removal. The removal of arsenic by non-magnetic nanoparticles has shown promising results with nanocrystalline titaniumoxide [5,113-115], synthetic akageneite [116], and a fibrous ion

Table 2.4. Nanoadsorbents for removal of As(V) from water (modified from Paper II, Table 1).

Nanoadsorbent	Size (nm)	SSA (m^2/g)	Method of removal	Conditions								Ads. capacity (mg/g)	Ads. Isotherm	Refs.
				pH	C_o (mg/L)	C_e (mg/L)	Dose (g/L)	T (^oC)	t (h)	rpm	Sep[a]			
Crystalline TiO_2	6	330	Batch	7.0	-	45	1.0	amb	22	-	C	37.5	Freundlich	[5]
TiO_2 Degussa P25	-	50	Batch	6.3	0.0075-6.7	-	0.05	-	0.5	-	F	9.7	-	[114]
TiO_2: Hombikat UV 100 (99% anatase)	<10	334	Batch	4	-	-	-	-	2 - 3	-	-	-	Langmuir, Freundlich	[113]
Degussa P25 (~85% anatase, ~20% rutile)	~30	~55												
TiO_2	15	190-290	Batch	8.4	1	0.1	0.05-8		-	-	C	2.6	Freundlich	[115]
ZrO	20-30	35-45										2.4		
Fe_2O_3	5-25	50-245										0.8		
NiO	10-20	50-80										2.5		
TiO_2 aggregate nanoparticle media with organic and inorganic binders	-	50-150	Column Short Bed Adsorber (SBA)	7.9	0.028	-	-	-	0.5 min	-	-	-	-	
FIBAN-As[b]	HFO 10-20	-	Batch Column Pilot	7.7	-	-	-	20±2	24	-	-	75.7	Langmuir	[117]
Crystal akageneite (β-FeO(OH))	2.6	330	Batch	7.5	5-20	-	0.5	25	24	160	F	120	Langmuir	[116]
Nanoscale zerovalent iron (nZVI)	30	25	Batch	3-7	1	-	0.1	-	-	-	-	-	-	[4]

Nanoadsorbent	Size (nm)	SSA (m^2/g)	Method of removal	Conditions								Ads. capacity (mg/g)	Ads. Isotherm	Refs.
				pH	C_o (mg/L)	C_e (mg/L)	Dose (g/L)	T (^oC)	t (h)	rpm	Sep[a]			
nZVI, Fe^o	-	-				12						-	-	[118]
NiFe	≥100		Batch	7.5	100	0.4	2.0	-	3	-	F	-	-	
PdFe	10-20					32						-	-	
Fe_3O_4	28	-										1.6	-	[120]
Mn_3O_4	25	-	Batch	4	0.5	-	2.5	-	1/4	-	C	0.2	-	
$MnFe_2O_4$	12	-										2.2	-	
Magnetite (Fe_3O_4)	< 50		Batch	9	0.1-2		5	25	3	4000	C	0.2	Langmuir	[121]
Maghemite (Fe_2O_3)	< 20	<50	Batch	7	1-4	-	1	25	2	125	-	4.6	Langmuir, Freundlich	[122]
	12	98.8		8.0			0.011		24		M	172.3		
Magnetite (Fe_3O_4)	20	60	Batch	8.0	0-33.7	-	0.1	-	24	-	F	5.9	Langmuir	[6,119]
	300	3.7		6.1			2.5		24		F	0.7		
	3.8	203.2					0.06					50.0		
Maghemite (Fe_2O_3)	12.1	90.4	Batch	3	1-11	-	0.1	23±2	50	200	M	25.0	Langmuir	Paper I
	18.4	51.0					0.25					16.7		

[a]C=Centrifuge; F=Filtration; M=Magnetic; [b] fibrous ion exchanger impregnated with nanoparticles of hydrated ferric oxide (HFO)

exchanger impregnated with nanoparticles of hydrated ferric oxide (FIBAN-As) [117]. With TiO_2 adsorbent, the effectiveness of photocatalyzed oxidization of As(III) to As(V) has also been studied [5,114]. A study with aluminium oxide nanopowder has also been accomplished, but the results have not been as promising as with Fe_2O_3, NiO, TiO_2, and ZrO_2 [115].

Zero-valent iron nanoparticles (Fe^0, nZVI) have received considerable attention for its potential applications in groundwater treatment. It is assumed that the reactivity of core-shell nanoparticles is driven by oxidation of the Fe^0 core, since the core consists of mainly metallic iron, whilst the shell consists mostly of iron oxides and hydroxides. Thus, nZVI exhibits characteristics of both iron oxides (e.g., as an adsorbent) and metallic iron (e.g., as a reductant) [89,97]. As an adsorbent, nZVI with a dose of 0.1 g/L has reached 100% removal efficiency at pH 3, 5, and 7 in 12 hours for 0.1 mg As(V) /L [4]. In another study, 88% of arsenate was removed in one hour with Fe^0, while modification with Ni (NiFe) improved the efficiency up to 100% [118].

Laboratory scale applications of magnetic nanoadsorbents

The magnetic nanoparticles applied successfully for arsenic removal are magnetite (Fe_3O_4) [119-121], Jacobsite ($MnFe_2O_4$) [120], and maghemite (γ-Fe_2O_3) [115,122,Paper I]. Table 2.4 shows that the highest arsenate adsorption capacity, 172.3 mg/g, was achieved with 12 nm magnetite (dose 0.011 g/L) at pH 8. Magnetite was a product of a laboratory synthesis where a mixture of FeO(OH), oleic acid, and 1-octadecene were heated and stirred in an elevated temperature (320°C) for the desired time [119,123]. Nanoparticles of 20 and 300 nm in size were commercial products and showed 30 and almost 200 times smaller adsorption capacities, respectively [6]. Moreover, magnetic separation with a high-gradient magnetic field column and particle recovery was successful with 12 nm particles, while larger particles were retained in the column, and recovery was not possible. It was speculated that these nanoparticles have a large magnetic moment that provides a remanent magnetization at zero field, thus increasing their interactions with the residual stray magnetic fields present in the column. The magnetic field dependence of 12 nm particle retention was also studied, and it was noted that with a magnetic field of 0.15 T, particle retention was 100% [6]. A desorption study of aforementioned particles were conducted only for larger ones. It was observed that both particles regeneration was irreversible, As(V) was desorbed 20-25% and only about 1% with 300 nm and 20 nm particles, respectively. Competitive sorption was studied with lake water with 0.01 M $NaNO_3$ electrolyte solution as a reference. As(V)

adsorption decreased in the lake sample, which was probably due to the competitive adsorption with natural organic matter (NOM) [6].

As(V) adsorption on maghemite has been studied with both commercial [115] and laboratory synthesized nanoparticles [122]. With commercial maghemite, As(V) adsorption capacity was 0.8 mg/g at pH 8.4 and 3.8 mg/g at pH 6.7 [115]. An electrochemical synthesis was applied for laboratory synthesized maghemite. There, nanoparticles were cathodically electrodeposited (i.e., constant applied current density) from 0.01 M $FeCl_3$ solution at 20°C and pH 2 with a stainless steel sheet as cathode and a steel rod as anode. The current densities were varied from 500 mA/cm² to 2000 mA/cm². Arsenate adsorption capacity of 4.6 mg/g at pH 7 was detected [122].

Industrially manufactured nanoadsorbents

Examples of commercially available nanoadsorbents/filters suitable for water treatment are shown in Table 2.5. Companies selling and manufacturing these products are mainly from the United States. Turbo Beads and Saehan Industries are exceptions. Turbo Beads is based in Switzerland and Saehan Industries is based in Korea. Nanomesh [124], nanofiltration [125], and nanofibrous filters [126,127] are listed here under nanoadsorbents, since adsorption occurs at some stage during the purification process. Self-assembled monolayers on mesoporous support (SAMMS®) has been developed by the U.S. Pacific Northwest National Laboratory (PNNL) [128,129], and it is sold and marketed by two companies, Battelle and Steward Advanced Materials.

Iron-based commercial nanoadsorbents include ArsenX® [126,130], Bayoxide® E33 [131], and TurboBeads EDTA [132]. The technical fact sheet for Bayoxide® E33 does not mention nano [133], but in other instances, it has been mentioned that the pores of surface media are nanosize [112].

Turbo Beads EDTA is a member of a larger product family of magnetic products manufactured by Turbo Beads. Turbo Beads manufactures highly magnetic, chemically stable functionalized nanoparticles suitable for biochemical, medical, and chemical applications. Their most recent product development has resulted in nanomagnets for the removal of heavy metal

Table 2.5. Point-of-use (POU) nanotechnology-based technologies for removal of As(V) from water.

Technology		Description of nanomaterial	Manufacturer or organization	Link	Refs.
Type	**Based on**[a]				
Nanomesh -filters -waterstick	PSE A	Composed of carbon nanotubes that are bound together and placed on a flexible, porous substrate. The nanotubes can be placed on a flat or rolled substrate.	Seldon Technologies	http://www.seldontech.com	[124]
Nanofiltration -membranes -devices	F	Membrane filter with pore size of 0.1 to 10 nm is used as the main filtering section.	Saehan Industries Inc.	http://www.saehan.com/	[125]
Nanofibrous Alumina Filters -NanoCeram®	A F	Nanofibrous adsorbent technology with its line of filter media and cartridge filters, which are made with electropositive alumina nanofibers on a glass filter substrate.	Argonide Corporation	http://www.argonide.com/	[126]
Nanofiber - Fact®Media	A F	A gravity-flow filtration device, in which filter medium consists of a prefiltration layer that removes dirt, an adsorption layer that removes chemical contaminants and a nanofiber layer that removes colloidal-sized particles and contaminants.	KX Technologies	http://www.kxtech.com/	[127]
Self-Assembled Monolayers on Mesoporous Supports - SAMMS®	A	Glass or ceramic material with nanoscale pores to which a monolayer of molecules can be attached. Both the monolayer and the mesoporous support can be functionalized to remove specific contaminants.	The U.S. Pacific Northwest National Laboratory (PNNL); Battelle; Steward Advanced	http://www.pnl.gov/ http://www.battelle.org/ http://www.stewardmaterials.com/www	[128,129]
ArsenX®	A/IE	An adsorbent resin made of hydrous iron oxide nanoparticles on a polymer substrate.	SolmeteX	http://www.solmetex.com/water.html	[126,130]

Technology		Description of nanomaterial	Manufacturer or organization	Link	Refs.
Type	**Based on**[a]				
Titanium Oxide Nanoparticle Adsorbent -Adsorbsia™GTO™	A	Granular adsorptive media that removes arsenic from water through the combined oxidative and adsorptive properties of titanium oxide.	Dow Chemical Company	http://www.dow.com	[134]
Nanostructured Iron Oxide Adsorbent - Bayoxide® E33	A	A dry, granular nanostructured iron oxide media which combines the catalytic and adsorptive properties of iron oxide.	Adedge Technologies,Inc. Severn Trent Services	http://www.adedgetech.com http://www.severntrentservices.com/	[131]
TurboBeads EDTA	A	TurboBeads EDTA are highly magnetic nanoparticles with diameters less than 50 nm. The surface of the particles is covalently functionalized with EDTA equivalent groups (>0.1 mmol/g, immobilized DTPA) and can be used for the binding of heavy metals.	Turbo Beads	www.turbobeads.com	[132]

[a]PSE = particle size exclusion, A = adsoption, F = filtration, IE = ion-exchange

ions from water. These carbon coated iron-based nanomagnets were functionalized with ethylene diamine tetra-acetic acid (EDTA) to remove cadmium, lead, and copper from water [95]. Lead and cadmium (initial concentration 1 mg/L) were removed nearly to the regulated limit (Pb^{2+}: 15 µg/L; Cd^{2+}: 5 µg/L) within 5 minutes of contact time at pH 6 with an EDTA-nanomagnet dose of 0.5 g/L. The separation of EDTA-nanomagnets was conducted with a neodymium-based hard magnet with a surface magnetization of 1.3 T in 20 seconds [95]. The company claims that with little alteration of the nanomagnets, arsenic recovery could also be possible [132].

Nanoadsorbents described in Table 2.5 are at least capable of treating water at the point-of-use (POU) level. NanofiberFact®Media, ArsenX®, AdsorbsiaGTO™ [134], and Bayoxide®E33 can also treat water at the community scale level. Moreover, ArsenX®, and SAMMS® are suitable for industrial waste streams purification [112]. Based on the manufacturers' information, among these nanoadsorbents only SAMMS® and ArsenX® are moderately difficult to use and may need trained personnel. The rest of the nanoadsorbents were easy to use and to operate and maintain by unskilled personnel. The costs of the treatment units are difficult to estimate, and therefore exact amounts are not reported. All of the companies except Saehan Industries state that it is possible to retrofit a unit. The price of the filter/media is more available; however, the comparison between media can still be difficult and the price assumes mass production of the media. Table 2.6 summarizes the available costs of nanoadsorbents.

Table 2.6. Cost of filter/media of nanoadsorbents [112]

Nanoadsorbent	**Cost (US$)**	**Cost (€)[a]**
Nanomesh	unspecified	unspecified
Nanofiltration	unspecified	unspecified
Nanofibrous filters -NanoCeram® -Fact®Media	 3.00 /m² media 0.80-0.90	 2.30 /m² media 0.61-0.69
SAMMS®	150 /kg	114.80 /kg
ArsenX®	0.07-0.20 /1000 L	0.055 -0.15 /1000 L
Adsorbsia™GTO™	14 /L media	10.71 / L media
AD33	8-13 /L; 50 -> cartridges	6 – 10 /L; 38 -> cartridges
TurboBeads EDTA	unspecified	unspecified

[a]currency conversion unit 1 $ = 0.765 € (28.12.2011)

3. MATERIALS AND METHODS

The research in this thesis is focused on the preparation of maghemite nanoparticles and the study of their suitability for arsenate removal in laboratory scale experiments. Research consists of preparation of maghemite nanoparticles and their characterization, both qualitative and physical properties, study of adsorption and desorption kinetics, investigation of arsenate adsorption properties on maghemite, such effects as pH, surface area and competing ions, determination of adsorption mechanism, and evaluation of maghemite stability and regeneration properties.

Research was conducted with three different maghemites, sol-gel, mechanochemical, and commercial. Among studied maghemites, sol-gel maghemite was the main research target; the others were studied for reference. Thus the effect of different synthesis method and particle size on adsorption was evaluated. Sol-gel maghemite is known to be a fast and easily repeatable method, and it had been successfully synthesized for Cr(VI) removal [15]. Therefore, it was chosen to be the main maghemite to study.

3.1 Preparation of maghemite nanoparticles

Crystal magnetic γ-Fe_2O_3 nanoparticles (maghemite) were obtained from three different sources: commercial maghemite purchased from Sigma-Aldrich, synthesized by the mechanochemical method (mechanochemical maghemite, 3.1.1), and synthesized by the sol-gel method (sol-gel maghemite, 3.1.2).

3.1.1 Mechanochemical synthesis

In mechanochemical synthesis [91], solid reactants were mechanically mixed together by grinding, which proceeds to the final product with the following reactions (Formulas 3.1-3.2):

$$2\ FeCl_3 \cdot 6\ H_2O(s) + FeCl_2 \cdot 4\ H_2O(s) + 8\ KOH\ (s) \rightarrow 8\ KCl(s) + Fe_3O_4(s) + 14\ H_2O(g) \quad (3.1)$$

$$4\ Fe_3O_4\ (s) + O_2\ (g) \rightarrow 6\ \gamma\text{-}Fe_2O_3\ (s) \quad (3.2)$$

Powders of $FeCl_3 \cdot 6\ H_2O$ (1.35 g), $FeCl_2 \cdot 4H_2O$ (0.50 g), and KCl (3.9 g) were mixed together in mortar and pestle (porcelain) and ground for 30 minutes at ambient temperature in air. After 30 minutes of grinding, 1.22 g of KOH powder was added to a formed yellow paste and grinding continued for another 30 minutes. Synthesized nanoparticles were sonicated and washed with ultrapure water several times to obtain chloride-free particles. Separation of washed particles was conducted with a centrifuge (Sorvall^R RC26 plus; Sorvall Instruments, Dupont, Wilmington, DE) at 2000 rpm for 10 min and a vacuum filtering system with a membrane of 0.1 μm pore size (MF-Millipore membrane filter, mixed cellulose esters). Finally, the maghemite was dried in a vacuum oven at 50°C for 6 hours.

3.1.2 Sol-gel synthesis

Sol-gel synthesis of maghemite nanoparticles was slightly modified from the existing method [15]. Synthesis was a two-step method: first, magnetite (Fe_3O_4) was synthesized (Formula 3.3), and secondly, it was oxidized to maghemite ($\gamma\text{-}Fe_2O_3$) (Formula 3.4). Black precipitate of magnetite was produced when appropriate amounts of Fe(II) and Fe(III) salts in alkaline solution were mixed under nitrogen atmosphere. Oxidation of magnetite to maghemite was conducted by calcination at 250°C for 3 hours.

$$2\ Fe^{3+} + Fe^{2+} + 8\ NH_3 + 4H_2O \rightarrow Fe_3O_4\ (s) + 8\ NH_4^+ \quad (3.3)$$

$$4\ Fe_3O_4\ (s) + O_2\ (g) \rightarrow 6\ \gamma\text{-}Fe_2O_3\ (s) \quad (3.4)$$

In magnetite synthesis, 200 ml of double deionized water was deoxygenated by N_2 bubbling and mechanical stirring for 30 minutes. Then 5.2 g of $FeCl_3 \cdot 6\ H_2O$ and 2 g of $FeCl_2 \cdot 4\ H_2O$ were added with mechanical stirring. When iron salts were dissolved, 1.5 M NH_4OH was added drop by drop until the pH reached 10-11. Formed black magnetite precipitate was allowed to set gradually, and then it was washed 10-15 times with ultrapure water to obtain cleaned particles. Washed particles were collected with the help of an external magnet and freeze-dried (Edwards, Super Modulyo).

These dry particles were oxidized to maghemite with a continuous supply of compressed air at 250°C for 3 hours (Carbolite).

3.2 Characterization of maghemite nanoparticles

The structural characterization of maghemite nanoparticles was conducted by powder X-ray diffraction (XRD) for crystalline phase analysis (Philips PW1830). For verification of the crystalline phase and the composition of the synthesized product, Joint Committee on Powder Diffraction Standards files (JCPDS) were used for qualitative characterization. An X-ray photoelectron spectroscopy (XPS) was applied to verify the iron oxidation state and to evaluate the bond strength of iron and arsenate (PHI 5600). Transmission electron microscopy (TEM) image was performed to determine the particle size and morphology of maghemite nanoparticles as well as the crystallinity of sorbed species (JEOL, 2010 TEM). A gas adsorption analyzer with the multipoint Brunauer, Emmett, Teller (BET) method was used for a specific surface area determination (Quantachrome Autosorb-1). The magnetic properties of maghemite nanoparticles were examined by a vibrating sample magnetometer (VSM) with a 9T superelectromagnet (LakeShore 7037/9509-P). A point of zero charge, pH_{pzc}, was measured by a Zeta Plus analyzer (Brookhaven) and a Zetasizer Nano ZS analyzer (Malvern Instruments Ltd.). Fourier transform infrared spectroscopy (FTIR) was applied for molecular-level investigations (Perkin Elmer, Spectrum BX).

3.3 Concentration analysis of solutions

Total arsenic concentrations in the solutions were determined using inductively coupled plasma optical emission spectrometer (ICP-OES, Optima 3000XL, Perkin Elmer) and inductively coupled plasma-mass spectrometer (ICP-MS, Sciex Elan 6000, Perkin Elmer). A flow injection analyzer (FIA) was employed for analysis of phosphate (Foss FiaStar 5000). Silica concentrations were analyzed by ICP-OES (iCAP 6300, Thermo Electron Corporation). ICP-OES (Perkin Elmer) and ultraviolet-visible spectrophotometer (UV-VIS, UV-1201 Shimadzu) were applied for the iron concentration measurement.

3.4 Batch experiments

This section reports the batch experiments conducted in the research. The description of the experiments are divided into four parts according to the order of papers presented in this thesis: Adsorption isotherm, adsorption mechanism, desorption of As(V) and adsorbent recycling, and competing anions. All three maghemites – commercial, mechanochemical, and sol-gel – were studied in Papers I and II, while only commercial and sol-gel maghemite were studied in Papers III and IV. Mechanochemical maghemite was excluded from the experiments in Papers III and IV due to weaker magnetic properties compared to other maghemites and time-consuming preparation when washing off impurities from the synthesized product.

Adsorption isotherm

Adsorption batch tests were performed at room temperature (23 ± 2°C) with 200 rpm agitation (Flask Shaker, SF1, Stuart Scientific) and 50-hour equilibrium time. The use of equilibrium time of 50 hours is based on the results of adsorption kinetic study that was carried out at different time intervals under pH 5. The adsorption tests of mass/volume ratio for commercial, mechanochemical, and sol-gel maghemite were 0.25, 0.06, and 0.1 g/L, respectively. Adsorption isotherms were studied by varying the initial As(V) concentration (1–11 mg As(V)/L) and solution pH (3, 5, 7 and 9). The pH of the solutions was adjusted by 0.1 M NaOH or HNO_3 stock solutions. When the adsorption equilibrium was reached, the adsorbent was separated via an external magnet and the supernatant was collected for the metal analysis. Magnetic separation of maghemite nanoparticles was conducted by a hard magnet, Neodym (Neorem Magnets Oy). (Paper I).

Adsorption mechanism

For adsorption mechanism studies, the adsorption batch experiments followed the procedure described in the previous section (Paper I). After the adsorption experiment, the adsorbent was filtered out by a vacuum filtering system with a 0.1-µm filter membrane (MF- Millipore membrane filter, mixed cellulose esters). The filtrand was dried overnight at room temperature before measurements were taken (Paper II).

Desorption of As(V) and adsorbent recycling

Arsenate desorption from a commercial and sol-gel maghemite surface was investigated by three sets of experiments: (1) determination of the best alkaline desorption solution among 0.1 M NaOH, Na_2CO_3, Na_2HPO_4, NaHCO3, CH3COONa· $3H_2O$ (NaAc) solution, (2) investigation of the concentration effect of the best desorption solution by NaOH concentrations of 0.01, 0.1, 0.5, 1, and 2 M, (3) study of the desorption kinetics. All adsorption batch tests were performed at room temperature (23 ± 2°C) with 200 rpm agitation (IKA Lortechnik, KS 501 digital) and 50-hour equilibrium time at pH 3 with initial As(V) concentration of 3 mg/L. The mass/volume ratios for adsorption tests for commercial and sol-gel maghemite were 0.25 and 0.1 g/L, respectively. Desorption batch tests were performed at 23 ± 2°C with 200 rpm agitation and 50-hour equilibrium time. Desorption kinetics was accomplished with 0.1 M NaOH at different time intervals, from which the 50-hour equilibrium time was chosen. The mass/volume ratios used in desorption experiments were 0.2 g/L and 0.12 g/L for commercial and sol-gel maghemite, respectively. After the adsorption batch experiments the adsorbent was separated from the As(V) solution and rinsed three times with double-deionized water to remove residue As(V) and other possible impurities prior to the batch desorption experiments. With sol-gel maghemite, the separation was conducted with an external magnet, and the rinse water from the magnetic separation was vacuum-filtered to recover adsorbent possibly left in the water after rinsing. With commercial maghemite, the particle separation from water and rinsing procedure was accomplished using a vacuum filtering process. Due to the commercial maghemite's high dispersion property in water, which leads to weakening magnetic separation, only filtration was used for the commercial maghemite separation to make the rinsing procedure reliable and the desorption experiment repeatable. The filtrand was dried overnight at room temperature and then separated from the filter by spatula, weighed and used for the desorption experiment (Paper III).

The recycling properties of maghemites were studied with successive cycles of adsorption-desorption experiments. The adsorption experiments were conducted with three different initial As(V) concentrations: 0.5, 1, and 3 mg/L at pH 3 followed by a desorption using 1 M NaOH. An equilibrium time of 48 hours was applied for both the adsorption and desorption experiments since it is a more convenient time than 50 hours to perform sequential experiments. The two-hour lack in adsorption/desorption equilibrium time was confirmed not to have an effect on the results when compared to the 50-hour equilibrium time. The mass/volume ratios for

experiments were the same as stated in the previous section. The separation of the adsorbent, both for commercial and sol-gel maghemite, was conducted with a vacuum filter after each adsorption and desorption experiment. In each round of adsorption or desorption experiments, the adsorbent used was the dried filtrand. The change of separation technique from magnet to filtration with sol-gel maghemite was due to better time management when the experiments were conducted in successive cycles (Paper III).

Competing anions

The effect of anion competition on arsenate adsorption (0.5, 1, and 3 mg As(V)/L) was studied by sulphate (20 and 250 mg SO_4/L) and nitrate (1 and 12 mg NO_3-N/L) at pH3, and by phosphate (0.5, 1.5, and 2.9 mg PO_4-P /L) and silicate (10, 30, and 50 mg SiO_2/L) at pH 3 and 7 with commercial and sol-gel maghemite. The groundwater sample spiked with 0.5 and 1 mg As(V)/L was also investigated both at pH 3 and 7. Solutions applied in batch experiments were a mixture of As(V) and one competing ion at a certain concentration except in the case of the groundwater experiments. The blank experiments were run simultaneously with studied As(V) concentrations in double-deionised water at pH 3 and 7 with both adsorbents. A 50-hour equilibrium time and 200 rpm agitation at room temperature (23 ± 2°C) with a mass/volume ratio of 0.25 and 0.1 g/L for commercial and sol-gel maghemite, respectively, were applied for all experiments (Paper IV).

4. RESULTS AND DISCUSSION

4.1 Characterization of maghemite nanoparticles

Nanoparticles qualitative characterization was conducted by XRD and FTIR, which were also utilized for crystalline phase verification together with a TEM image. Along with composition verification was the iron oxidation state determined by XPS. VSM was employed to determine the magnetic properties of nanoparticles. A TEM image was also applied for morphology observation and particle-size determination, which are important characteristics of adsorbent materials together with specific surface area and surface potential.

4.1.1 Qualitative properties

The XRD pattern in Figure 4.1 confirmed that every studied nanoparticles crystal orientation belonged to maghemite.

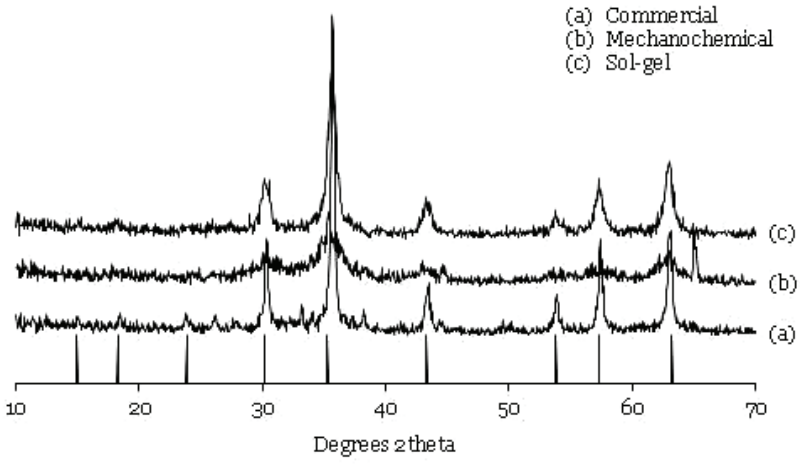

Figure 4.1. XRD patterns of commercial, mechanochemical, and sol-gel maghemite. (Paper I). Normalized standard peaks expressed in vertical peaks at positions (degrees 2 theta) 15.0, 18.3, 23.9, 30.2, 35.3, 43.3, 53.8, 57.3 and 63.2.

This was verified by comparing maghemites peak positions to the JCPDS standard configuration of maghemite (Figure 4.1). However, a difference in peak intensity and broadening was observed between maghemites. The XRD pattern of commercial maghemite possesses peaks with strong intensity and sharpness, followed by the slightly weaker and broader pattern of sol-gel maghemite. The broadest peaks with the weakest intensity are observed by mechanochemical maghemite. Change in XRD pattern intensity and peak broadening is explained by the decreasing particle size of the nanoparticles (Figure 4.4).

To exclude the existence of magnetite (Fe_3O_4) in particles, the oxidation state of iron was verified with XPS, which indicated that the electronic state of the iron in all maghemites was Fe^{3+}.

Figure 4.2 shows the FTIR spectra of different maghemites. Note that the commercial maghemite has a more detailed spectrum than the other two maghemites. This is due to the crystal order in atoms: the atoms in commercial maghemite crystals are well-ordered while the atoms in other maghemites are more strongly disordered. It is worth noting that the characteristic absorptions for all maghemites can be found at all spectra: two broad absorption bands at about 400 cm^{-1} and 600 cm^{-1} [135,136]. Moreover, well-ordered maghemites show typical shoulders in the regions of 402 cm^{-1}, 415 cm^{-1}, 440 cm^{-1}, 552 cm^{-1}, 580 cm^{-1}, 630 cm^{-1}, 692 cm^{-1}, and 725 cm^{-1} [135].

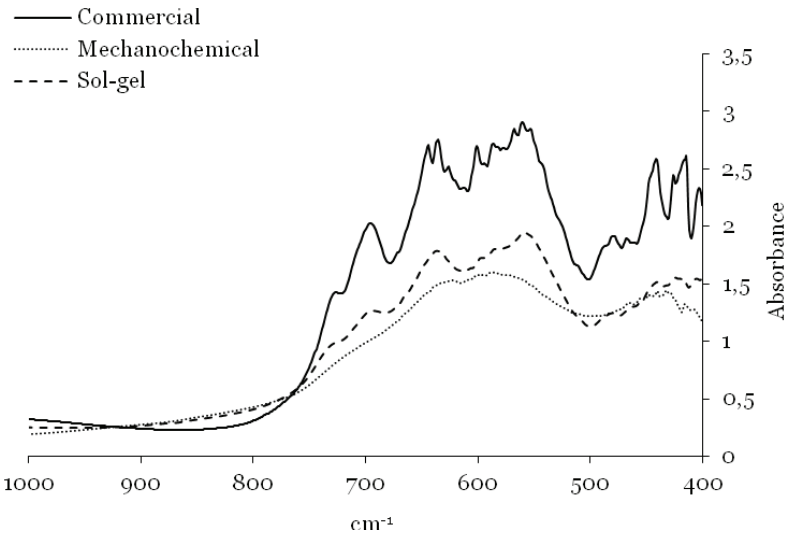

Figure 4.2. FTIR spectra of different maghemites. (Unpublished data)

Figure 4.3 shows the maghemites' magnetic behaviour under a strong magnetic field. None of the nanoparticles had the properties of a hard magnet, but all of them were paramagnetic material [63]. The magnetization curve of commercial maghemite showed slight hysteresis; thus, it is a weak ferromagnetic material. Superparamagnetic behaviour was observed with sol-gel and mechanochemical maghemite, which can occur with very small particles (~10 nm) [81]. All of these maghemites would be suitable for magnetic separation applications since they do not possess the quality of a hard magnet [55].

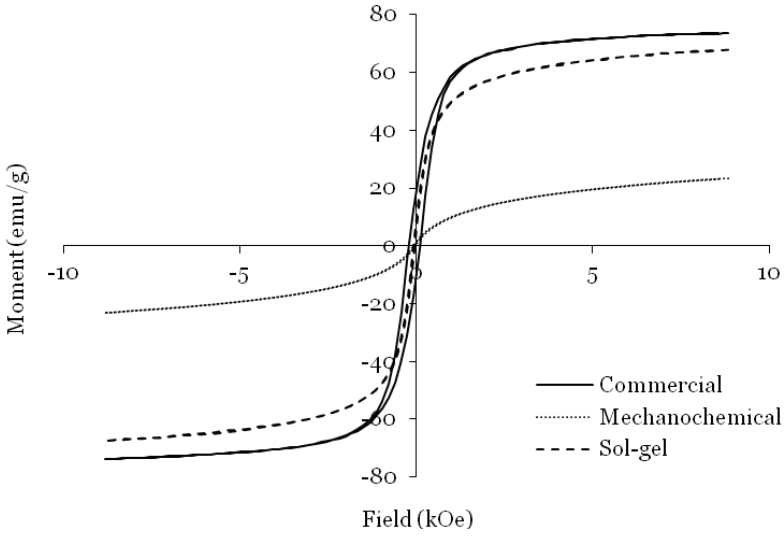

Figure 4.3. Magnetization curves of commercial, mechanochemical, and sol-gel maghemite at room temperature (23±2°C). (Paper I)

4.1.2 Physical properties

The following properties of three maghemites were investigated: particle size, particle size distribution, magnetization value, specific surface area, and surface potential (pH_{pzc}) (Paper I, Table 1). Mechanochemically synthesized maghemite nanoparticles are the smallest in particle size (3.8 nm) among the three maghemites studied. This was not only revealed by a particle-size calculation from the TEM image (Figure 4.4), but was also supported by the specific surface area (203.2 m^2/g), the smallest magnetization value at 5 kOe (19.6 emu/g), and the XRD pattern (Figure 4.1). The specific surface area of mechanochemical maghemite is 40 times

greater, almost 20 times greater with sol-gel and 10 times greater with commercial maghemite compared to the bulk product (5.05 m^2/g) [137].

Figure 4.4 illustrates the effect of particle-size dependence on the specific surface area and the magnetization value of different maghemites. The saturation magnetization value of commercial maghemite (71.7 emu/g) and sol-gel maghemite (64.3 emu/g) at 8-9 kOe is related to the literature value, which has a range of 60-80 emu/g [82]. The specific surface area of maghemites increases with declining particle size, as expected, because there is an inverse relationship between particle size and specific surface area [73]. Magnetization is known to decline when particle size decreases [138], which is also observed in Figure 4.3. An explanation of this behaviour could be the small-particle surface effect and the internal cation disorder [135]. However, the exact mechanism is still unknown.

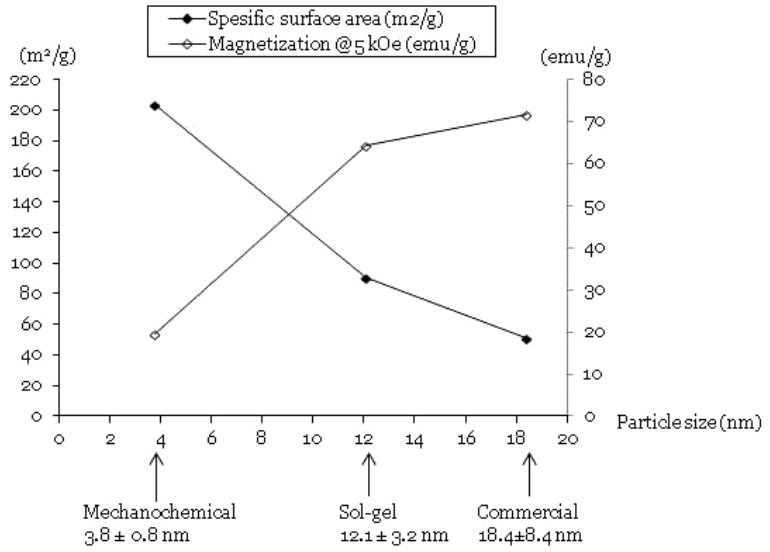

Figure 4.4. The effect on specific surface area and magnetization value of maghemites particle size.

Particle size and its distribution range expressed in Figure 4.4 were calculated from TEM images by measuring the diameter of 100 particles randomly chosen. Sol-gel and mechanochemical maghemite had the most even particle size distribution, which is a common observation with these synthesis methods [69,70]. Morphology differences between particles were discovered (Figure 4.5): hexagonal, spherical, and irregular shapes were observed with commercial, sol-gel, and mechanochemical maghemites,

respectively. This variety is thought to be due to the difference in synthesis methods.

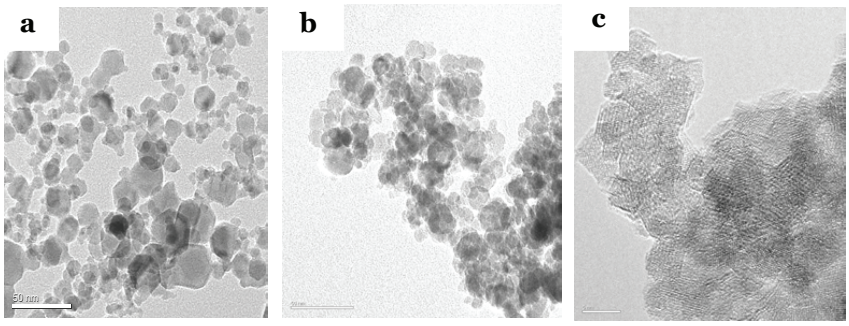

Figure 4.5. TEM image of commercial maghemite with a scale bar of 50 nm (a), sol-gel maghemite with a scale bar of 50 nm (b), and mechanochemical maghemite with a scale bar of 5 nm (c). (Paper I)

Zeta potential measurements conducted at a pH range of 3-10 revealed the pH_{zpc}, i.e., the pH value when the surface charge of maghemite particles is neutral. pH_{zpc} for commercial, mechanochemical, and sol-gel maghemite were 7.5, 5.7, and 5.7, respectively. Below the pH_{zpc} the maghemite surface is positively charged, and above the pH_{zpc} the maghemite surface is negatively charged [35]. Moreover, the absolute value of the zeta potential indicates the system stability. When the zeta potential value is higher than 25 mV, the system is stable, and repulsive forces between the particles are strong enough to keep particles dispersed [139]. Such high zeta potential values were measured at pH≤ 5 and pH ≥8.5 for all studied maghemites (Paper II, Figure 1).

4.2. Kinetics

4.2.1 Adsorption kinetics

Figure 4.6 shows the adsorption kinetics of three different maghemites. The plateau (equilibrium) of different maghemites is reached in the same time frame, around 30-50 hours. The kinetics of different maghemites follows the typical behaviour of heavy metal adsorption onto an oxide surface; the adsorption reaction is rapid at first, and then the rate gradually diminishes [35,140]. In 30 minutes, approximately 70%, 80%, and 90% of the arsenate has been adsorbed onto the mechanochemical, sol-gel, and commercial maghemite, respectively. The rapid reaction is normally interpreted as an

external diffusion process, while several possible explanations exist for a slow reaction stage: (1) formation of an inner-surface complex, (2) diffusion of the adsorbate into the adsorbent pores, or (3) a precipitation reaction [35,140].

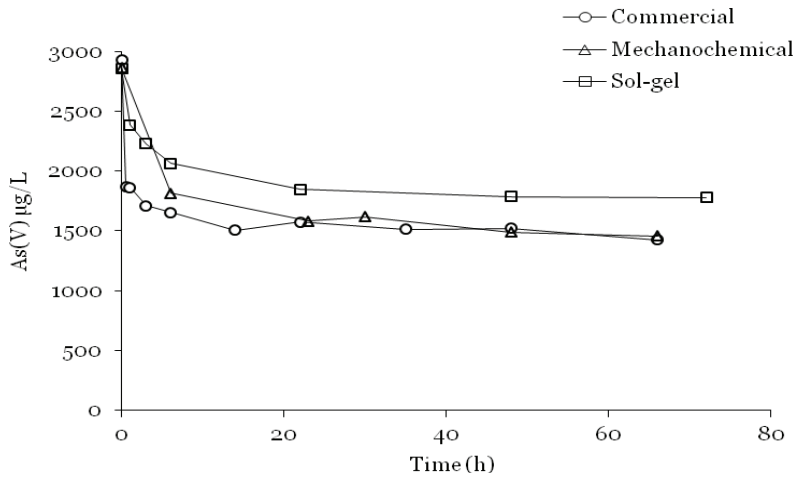

Figure 4.6. Adsorption kinetics of commercial (dose 0.25 g/L), mechanochemical (dose 0.06 g/L), and sol-gel maghemites (dose 0.1 g/L). Initial As(V) concentration 3 mg/L, pH 5. (Paper I)

To investigate the possible explanation for the slow reaction stage, adsorption kinetics was examined with different kinetic models, such as 1st order, 2nd order, the Elovich equation, parabolic diffusion, pseudo-first order, and pseudo-second order [35,141]. From these, the data fit best with the pseudo-second order kinetic model when correlation coefficient (R^2) value was evaluated (Figure 4.7). Also, the calculated q_e values agree very well with the experimental data, as can be seen in Table 4.1. The pseudo-second order model considers the rate-limiting step as the formation of inner-sphere surface complexes [141], which is also in agreement with the results observed from adsorption mechanism studies with maghemites (Paper II).

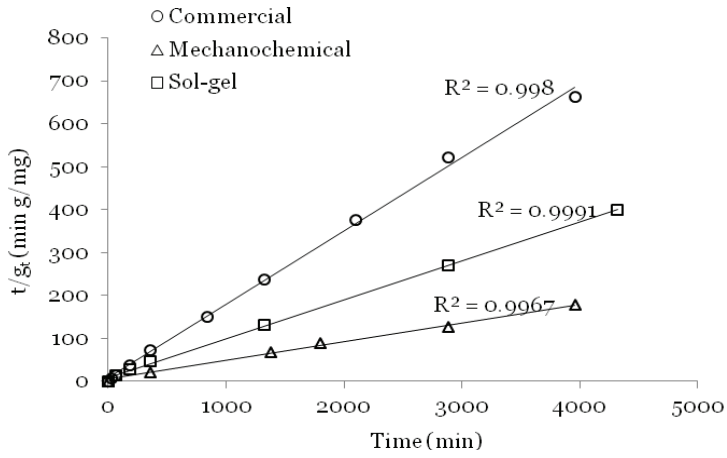

Figure 4.7. Pseudo-second order kinetic plots for arsenate adsorption with mechanochemical (unpublished data), sol-gel, and commercial maghemite (Paper III).

The kinetic rate constants (k_2) (which take into account the rate-limiting step of adsorption) and the initial sorption rate (h) are shown for mechanochemical, sol-gel, and commercial maghemite in Table 4.1. The kinetic rate is slowest with mechanochemical maghemite, followed by sol-gel and commercial maghemite. Commercial maghemite shows a kinetic rate nine times higher than that for mechanochemical maghemite and five times higher than that for sol-gel maghemite. In contrast, the initial sorption rate is the highest with mechanochemical, followed by commercial and sol-gel maghemite.

Table 4.1. Pseudo-second order rate constants for adsorption with mechanochemical (unpublished data), sol-gel, and commercial maghemite (Paper III).

	q_e, exp (mg/g)	**q_e, calc. (mg/g)**	**h (mg / (g min))**	**k_2 (g / (mg min))**	**R^2**
Mechanochemical	22.7	22.8	0.237	0.0005	0.997
Sol-gel	10.8	11.0	0.117	0.0010	0.999
Commercial	6.0	5.8	0.152	0.0045	0.998

The important characteristics of the adsorbent that determine equilibrium capacity and rate are surface area, the physicochemical nature of the surface, the availability of that surface to adsorb molecules or ions, the physical size, and form of the adsorbent particles [142]. Moreover, system parameters such as the pH, temperature, and agitation can also influence the adsorption as they affect one or more of the above parameters. In this study the pH, temperature, and agitation were kept constant and the same for all maghemites. Thus, one explanation for the difference in kinetic rates

of maghemites is the physical size and form of the maghemite particles as well as their physicochemical nature. Commercial maghemite possess the largest particles and well-ordered crystallinity. Moreover, the hexagonal form of the particles differs from sol-gel and mechanochemical maghemite.

4.2.2 Desorption kinetics

Desorption kinetics was studied with 0.1 M NaOH at varying contact times. NaOH was chosen for the desorption solution among following alkaline solutions: Na_2CO_3, Na_2HPO_4, $NaHCO_3$, and NaAc due to its best performance (Paper III). Desorption kinetics was studied with sol-gel and commercial maghemite. Figure 4.8 shows that arsenate desorption is rapid at first, and then the rate gradually diminishes. Maghemites reached equilibrium in 24 to 50 hours with 80-90% desorption efficiency. Nearly 60% of arsenate was desorbed by commercial maghemite and 65% by sol-gel maghemite in one hour. Desorption kinetics is similar to adsorption kinetics, both in equilibrium time and in graph shape.

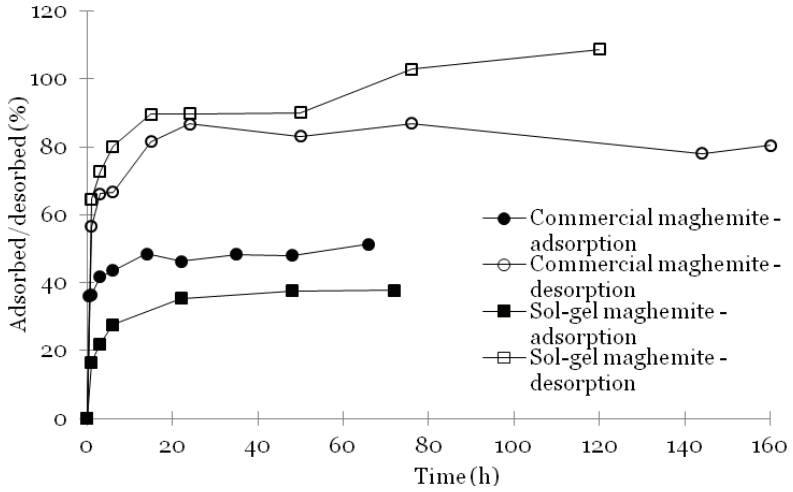

Figure 4.8. Adsorption and desorption kinetics of commercial and sol-gel maghemites.

Also, the data of desorption kinetics fit the best with the pseudo-second order model (Paper III, Figure 4), the initial sorption rate showing higher values in desorption than in adsorption for both maghemites (Paper III, Table 3). This indicates that arsenate desorption from the maghemite surface is faster than its adsorption onto a surface. This is possible due to a different bond formation in adsorption (bidentate binuclear) and

desorption (monodentate), as well as the level of surface coverage of maghemite.

4.3 Arsenate adsorption on maghemite nanoparticles

4.3.1 Effect of pH and surface area

Experimental data of adsorption isotherms fit well with the Langmuir isotherm (Paper I), indicating that the surface of maghemites was homogeneous and the adsorbed As(V) molecules formed a monolayer onto the maghemite surface. The pH employed in experiments was effectively the adsorption pH because the initial (adjusted) pH and final pH at the equilibrium were comparable. The adsorption capacity of different maghemites was clearly pH-dependent, and the most efficient adsorption occurs at pH 3 for all maghemites: 50.0 mg/g for mechanochemical, 25.0 mg/g for sol-gel, and 16.7 mg/g for commercial maghemite. Moreover, maximum adsorption capacity values declined in agreement with the specific surface area – the highest adsorption capacity with the largest specific surface area. Figure 4.9 illustrates the specific surface area and pH effect of different maghemites.

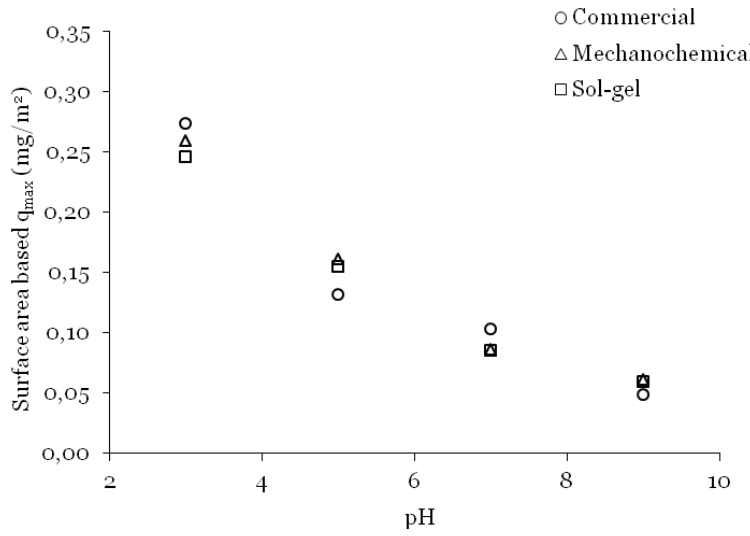

Figure 4.9. Surface area based As(V) adsorption maximum of different maghemites as a function of pH with initial As(V) concentration of 7 mg/L.

It is seen that surface area based adsorption maximums (q_{max}) are almost the same at different pH values as they are between different maghemites. This is logical and indicates that all three materials have approximately the

same surface density of binding sites with a similar pH response (i.e., Brönsted acidity of the binding sites is similar in all three materials). The pH dependence is closely related to the surface charge status of the nanoparticles at various pH values.

The maximum adsorption capacities are difficult to compare due to differences in experimental conditions. However, the comparison of results reported here and with some conventional adsorbents (Table 4.2) and other nanoadsorbents (Table 2.4) for arsenate removal with batch experiments gives an idea about the removal capability of the studied adsorbents. With conventional adsorbents, ferrihydrite and mesoporous alumina are showing higher adsorption capacity compared the studied maghemites. The reported adsorption capacity of activated alumina in column experiments ranges from 3 to 112 mg/g [29]. Among nanoadsorbents a few adsorbents (such as TiO_2, magnetite, and crystal agageneite) overcome the maghemite's adsorption capacity. In general, the maghemites' capability to adsorb arsenate is on a satisfactory level.

Table 4.2. The maximum adsorption capacity of some conventional adsorbents for the removal of As(V) from natural and drinking water with batch experiments.

Adsorbent	**pH**	**Conc./ range (mg/L)**	**Ads. dose (g/L)**	**SSA (m^2/g)**	**T (°C)**	**Capacity (mg/g)**	**Refs.**
Ferrihydrite	4.6	20-2000	2	202	-	149.8	[143]
Activated alumina grains	5.2	2.85-11.5	1-5	116-118	25	15.9	[144]
Mesoporous alumina	5	7.5-1500	5	307	20-25	121	[145]
Hematite	4.2	1-10	-	14.4	30	0.20	[146]
Goethite	9.0	0-60	1.6	39	22	4.0	[147]
Maghemite Commercial	3	1-11	0.25	51.0	23±2	16.7	Paper I
Mechano-chemical	3	1-11	0.06	203.2	23±2	50.0	
Sol-gel	3	1-11	0.1	90.4	23±2	25.0	

4.3.2 Effect of competing ions

The effect of sulphate (SO_4) and nitrate (NO_3-N) at pH 3, phosphate (PO_4-P) and silicate (SiO_2) at pH 3 and 7, on arsenate adsorption onto maghemite was investigated by sol-gel and commercial maghemite. Moreover, the combined effect of ions and other water characteristics on arsenate adsorption capacity were examined with a natural groundwater sample spiked with a certain amount of arsenate (Paper IV). In order for an ion to

compete for the same binding sites with arsenate, it should possess the same adsorption mechanism (i.e., inner-sphere surface complex) [43]. Another ion can also affect arsenate adsorption by steric effects, thus inhibiting the arsenate attachment onto the maghemite surface or by affecting the surface potential [44].

Sulphate and nitrate

Sulphate and nitrate were observed to have an insignificant effect on arsenate adsorption capacity with both maghemites at pH 3 (Tables 4.3 and 4.4, Paper IV). Such a result was somehow expected since nitrate adsorbs most likely by outer-sphere surface complexation [35], while sulphate may form both outer- and inner-sphere complexes [148].

Silicate

Silicate was observed to have the most effect on arsenate adsorption capacity at pH 7 with elevated silicate concentrations (Tables 4.3 and 4.4, Paper IV) with both maghemites. Slight silicate inhibition was observed with sol-gel (30 and 50 mg SiO_2/L) and commercial maghemite (50 mg SiO_2/L) with 3 mg As(V)/L at pH 3.

Silicate differs from arsenate and phosphate in chemical properties since it is capable of polymerization at high concentrations (≥ 60 mg/L) at pH 4 and even small concentrations (starting from 6 mg/L) at pH 6 and 7 [46,149]. Polymerization is the possible explanation for the increase in silicate inhibition with elevated silicate concentration and pH. Polymeric species can coat more of the surface and the adsorption sites on the adsorbent surface than monomeric silica, thus inhibiting As(V) adsorption by steric effects or by decreasing the surface potential [44].

Phosphate

The phosphate competing effect on arsenate adsorption capacity increases with elevated phosphate concentrations at both pH values and adsorbents (Tables 4.3 and 4.4, Paper IV).

Table 4.3. The effect of competing ions on As(V) adsorption capacity (mg/g) with sol-gel maghemite at pH 3 and pH 7.

pH 3			pH 7		
Initial As(V) mg/L	**Anion (mg/L)**	**Adsorption capacity As(V) mg/g**	**Initial As(V) mg/L**	**Anion (mg/L)**	**Adsorption capacity As(V) mg/g**
	SO_4			***SO_4***	
0.5	0	4.7	0.5	0	-
	20	4.7		20	-
	250	4.6		250	-
	NO_3-N			***NO_3-N***	
0.5	0	4.7	0.5	0	-
	1	4.8		1	-
	12	4.6		12	-
	PO_4-P			***PO_4-P***	
0.5	0	4.7	0.5	0	3.6
	0.5	4.6		0.5	2.5
	1.5	4.6		1.5	1.6
	2.9	4.1		2.9	0.7
1.0	0	9.4	1.0	0	4.0
	0.5	8.6		0.5	3.1
	1.5	7.7		1.5	2.4
	2.9	6.7		2.9	1.7
3.0	0	18.2	3.0	0	5.7
	0.5	16.2		0.5	5.1
	1.5	12.9		1.5	4.4
	2.9	12.0		2.9	3.9
	SiO_2			***SiO_2***	
0.5	0	4.7	0.5	0	3.6
	10	4.7		10	2.7
	30	4.9		30	2.4
	50	4.7		50	2.8
1.0	0	9.4	1.0	0	4.0
	10	9.4		10	3.7
	30	9.5		30	3.0
	50	9.7		50	3.2
3.0	0	18.2	3.0	0	5.7
	10	18.3		10	5.1
	30	16.7		30	4.2
	50	16.2		50	4.3
	Ground water			***Ground water***	
0.5	0	4.7	0.5	0	3.6
	*	4.8		*	3.4
1.0	0	9.4	1.0	0	4.0
	*	8.6		*	4.8

*see Paper IV, Table 3 for water quality results

Table 4.4. The effect of competing ions on As(V) adsorption capacity (mg/g) with commercial maghemite at pH 3 and pH 7.

pH 3			pH 7		
Initial As(V) mg/L	**Anion (mg/L)**	**Adsorption capacity As(V) mg/g**	**Initial As(V) mg/L**	**Anion (mg/L)**	**Adsorption capacity As(V) mg/g**
	SO_4			***SO_4***	
0.5	0	1.9	0.5	0	-
	20	1.8		20	-
	250	-		250	-
	NO_3-N			***NO_3-N***	
0.5	0	1.9	0.5	0	-
	1	1.9		1	-
	12	-		12	-
	PO_4-P			***PO_4-P***	
0.5	0	1.9	0.5	0	1.7
	0.5	1.8		0.5	1.2
	1.5	1.7		1.5	0.8
	2.9	1.2		2.9	0.4
1.0	0	3.8	1.0	0	2.2
	0.5	3.3		0.5	1.5
	1.5	2.8		1.5	1.1
	2.9	2.4		2.9	0.9
3.0	0	6.8	3.0	0	3.7
	0.5	6.4		0.5	2.6
	1.5	5.6		1.5	2.0
	2.9	5.2		2.9	1.5
	SiO_2			***SiO_2***	
0.5	0	1.9	0.5	0	1.7
	10	1.9		10	1.6
	30	2.0		30	1.3
	50	1.9		50	1.1
1.0	0	3.8	1.0	0	2.2
	10	3.8		10	2.2
	30	3.9		30	1.8
	50	3.9		50	1.6
3.0	0	6.8	3.0	0	3.7
	10	6.7		10	2.8
	30	6.8		30	2.7
	50	6.3		50	2.5
	Ground water			***Ground water***	
0.5	0	1.9	0.5	0	1.7
	*	1.9		*	1.7
1.0	0	3.8	1.0	0	2.2
	*	3.4		*	2.8

*see Paper IV, Table 3 for water quality results

When examined the decrease in As(V) adsorption capacity (in per cent) as a function of increasing arsenate concentration with a certain phosphate concentration, it is seen from Figures 4.10 and 4.11 that with both maghemites the decrease in arsenate adsorption capacity is more prominent at pH 7 than 3. Moreover, in general, phosphate inhibits slightly more arsenate adsorption onto commercial maghemite than onto sol-gel maghemite. With sol-gel maghemite, the decrease in As(V) adsorption capacity gradually increases with elevated arsenate concentration at pH 3, but the opposite situation is observed at pH 7 (Figure 4.10, graph (b)). In case of commercial maghemite, the phosphate effect is similar to sol-gel at pH 7, while at pH 3 it shows the highest As(V) adsorption capacity decrease with 1 mg As(V)/L (Figure 4.11 graph (a)).

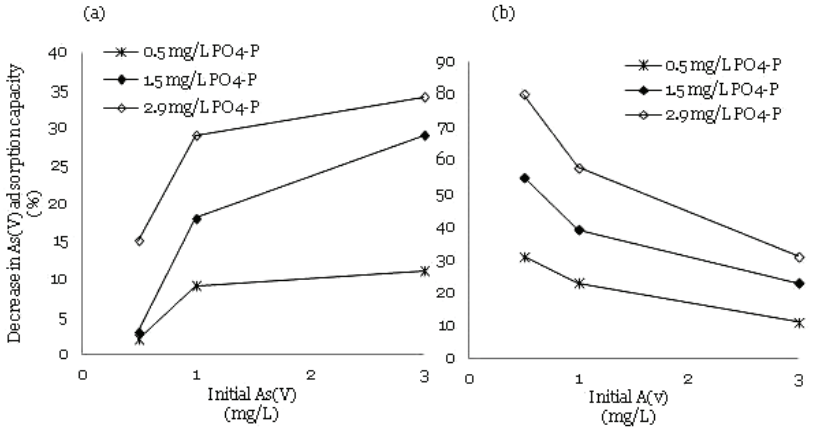

Figure 4.10. Phosphate effect on As(V) adsorption capacity decrease (%) at (a) pH 3 and (b) pH 7 with sol-gel maghemite.

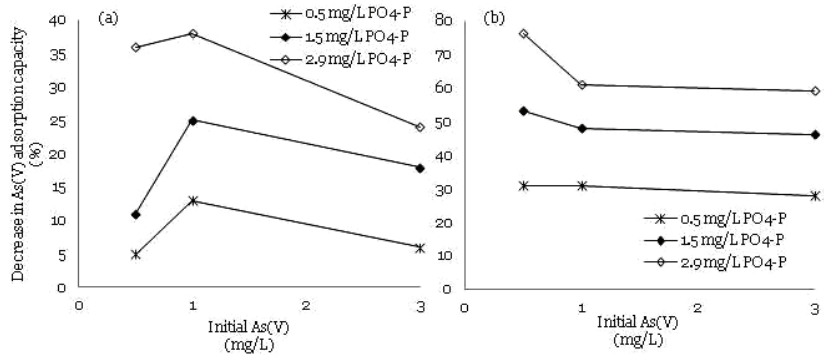

Figure 4.11. Phosphate effect on As(V) adsorption capacity decrease (%) at (a) pH 3 and (b) pH 7 with commercial maghemite.

The phosphate competing effect is influenced by the pH, which has an effect on phosphate and arsenate speciation as well as the electrostatic charge at the adsorbent surface [43]. Moreover, anion(s) concentration and the amount of available binding sites on maghemite surface determine the level of the competition between these two anions. In the previous section (4.3.1), it was stated that sol-gel and commercial maghemite have the same surface density of binding sites with similar pH response. Therefore, enhancing competition with elevated phosphate concentrations could be the result of decreasing the amount of surface sites on the maghemite surface. This explanation is possible in pH 3 when an increase in arsenate concentration causes a gradual decrease in the As(V) adsorption capacity with sol-gel maghemite (Figure 4.10, Graph (a)). In case of commercial maghemite, 1 mg As(V)/L shows a higher decrease in As(V) adsorption capacity than other concentrations. The reason for this behaviour is not known.

At pH 7, the phosphate competition is higher than at pH 3, which is more likely due to change in the maghemite's surface charge to negative (pH > pH_{pzc}, Paper I, Table 1), which decreases the available binding sites and enhances anions competition [150]. The surface area based maximum As(V) adsorption capacity, q_{max} (mg/m^2), is threefold smaller at pH 7 than at pH 3, which also indicates that maghemite's adsorption capacity is diminished at pH 7 (Paper I). The decrease in As(V) adsorption capacity was at its highest with small arsenate concentrations at pH 7 with both maghemites. This is possible due to the small amount of active surface sites that are negative in charge and the change in bonding from bidentate to monodentate in the case of arsenate (Paper II). Therefore arsenate is more freely released to the solution and replaced by phosphate.

Groundwater

The results of adsorption capacities of arsenate from the laboratory and groundwater are shown in Tables 4.3, 4.4, and Paper IV for sol-gel and commercial maghemite. The results reveal that both adsorbents behave similarly. Arsenate adsorption capacity was not affected at the studied pH values with 0.5 mg As(V)/L in groundwater, whereas the discrepancy of adsorption results with 1 mg As(V)/L is noticeable at pH 3 and pH 7. At pH 3, the arsenate adsorption capacity decreases by 0.8 and 0.4 units, while at pH 7 it increases by 0.8 and 0.6 units with sol-gel and commercial maghemite, respectively, when compared with laboratory water spiked with As(V).

When dealing with natural water, one of the potential factors inhibiting arsenate adsorption is natural organic matter (NOM), which mainly consists of humic and fulvic acids (HA; FA). NOM is a large, complex molecule which has multiple anionic functional groups with differing dissociation constants [151]. The arsenate adsorption capacity decrease at pH 3 with 1 mg As(V)/L is possible due to NOM inhibition, while with 0.5 mg As(V)/L, NOM inhibition does not exist since maghemite has presumably a sufficient amount of active surface sites to adsorb. The increase in arsenate adsorption capacity at pH 7 could be explained by the combined effect of silicate and bicarbonate [152] or an ionic strength effect (Paper II, Figure 2). It is supposed that negatively charged NOM is not influencing arsenate adsorption at pH 7 due to negative adsorbent surface (Paper I, Table 1; and Paper II, Figure 1), which lowers its attraction towards the maghemite surface. Moreover, FA forms a possible outer-sphere surface complex at pH 7, which is less favoured for competition with arsenate inner-sphere surface complexes [153].

4.4 Adsorption mechanism

The As(V) adsorption mechanism onto three different kinds of maghemite nanoparticles were studied by macroscopic characterization (zeta potential measurement, ionic strength effect) and microscopic characterization (FTIR, XPS, XRD, TEM).

A point of zero charge, pH_{pzc}, for different nanoparticles was estimated graphically by zeta potential measurements (Paper II). It was observed that pH_{pzc} decreased gradually with sol-gel and commercial maghemite with increasing As(V) concentration onto the maghemite nanoparticle (Table 4.5). With mechanochemical maghemite, a pH_{pzc} decrease was noticed, but only with the highest As(V) loading. However, the increase of pH_{pzc} at 2 mg/L may be caused by experimental inaccuracy. The shift in pH_{pzc} with increasing As(V) concentration is assumed to be a result of inner-sphere complex formation, which changes the surface charge of the particle [154].

Table 4.5. The effect of As(V) concentration on pH_{pzc} with different maghemites.

As(V) concentration	**pH_{pzc} of maghemites**		
(mg/L)	*Mechanochemical*	*Sol-gel*	*Commercial*
0	5.7	5.7	7.5
2	6.5	4.6	5.4
8			4.1
11	3.6	4.0	

The ionic strength effect on As(V) adsorption was studied by 0.01 M and 0.1 M $NaNO_3$ and 8 mg/L of As(V) concentration (Paper II, Figure 2). At pH 3, the percentage of As(V) removed in both ionic strength solutions was approximately 40, 30, and 40 for commercial, sol-gel, and mechanochemical maghemite, respectively. A different ionic strength effect on As(V) adsorption was the following – As(V) removal efficiency either stayed equal or increased slightly, but did not decrease. Since outer-sphere surface complex formation would lead to a decrease in removal efficiency, due to electrostatic interactions [155], it is clearly not the case in this study. Consequently, the result of ionic strength effect indicated inner-sphere surface complex formation in adsorption.

A molecular scale investigation was conducted by FTIR for both a 0.5 M As(V) solution at different pH (speciation) and solid maghemites with and without As(V) adsorption (Paper II, Figures 3-5). Table 4.6 summarizes the characteristic absorption wavenumbers of As(V) speciation.

Table 4.6. Characteristic absorption wavenumbers of 0.5 M As(V) at different pH.

0.5 M As(V)	Arsenic speciation	Absorption peak, (cm^{-1})	Absorption peak, (cm^{-1})	Absorption peak, (cm^{-1})
pH3	$H_2AsO_4^-$		877 (s, sm)[b]	907 (s)
pH5	$H_2AsO_4^-$		877 (s, sm)	907 (s)
pH7	Mixture of $H_2AsO_4^-$/ $HAsO_4^{2-}$	860 (s)[a]		907 (w)[c]
pH9	$HAsO_4^{2-}$	859 (s)		

[a] small; [b] small, smaller than 907 cm^{-1} adsorption; [c] weak

Single absorption at 859 cm^{-1} corresponds to the ν_{as} (As-O) of $HAsO_4^{2-}$, and absorption at 907 cm^{-1} is ν_{as} (As-O) of $H_2AsO_4^-$. At pH 3 and pH 5, the $H_2AsO_4^-$ is split into two peaks, where 877 cm^{-1} corresponds to ν_s(As-O) and 907 cm^{-1} is the same as in pH 7, but with stronger absorption. Absorption wavenumbers of protonated As(V) species are in agreement with previous studies [154,156-158]

Table 4.7 shows the absorption wavenumbers of As(V) adsorbed maghemites. Different absorption positions and splitting of bands were observed compared to dissolved species. This indicates inner-sphere complex formation on the surface, because in an outer-sphere surface complex, the protonated forms exhibit spectra at similar band positions as dissolved As(V) species at a specific pH [156].

Table 4.7. Absorption wavenumbers of As(V) adsorbed maghemites.

Maghemite	**Absorption, cm^{-1}**			
	pH 3	*pH 5*	*pH 7*	*pH 9*
Mechanochemical	830-834 (s)[a] 860-869 (sh,w)[b]	830-834 (s) 860-869 (sh,w)	830-834 (s) 860-869 (sh,w)	830-834 (s) 860-869 (sh,w)
Sol-gel	830-835 (s) 869 (sh,w)	826-835 (s)	826-835 (s)	826-835 (s)
Commercial	830-835 (s) 869 (sh, w)	826-835 (s)	826-835 (s)	826-835 (s)

[a]shoulder; [b]shoulder, weak

Absorption at 830 cm^{-1} (826-835 cm^{-1}, 830-834 cm^{-1}) indicates that ν_{as} (As-O) of 907 cm^{-1} at pH 3 and pH 5 and 859-860 cm^{-1} at pH 7 and pH 9 has shifted to a lower wavenumber when a metal- oxygen bond, (Fe-O-As) is formed. The shoulder at position 860-869 cm^{-1} is assigned to be another stretching vibration of As-O, which is an indication of a bidentate complex formation, $(FeO)_2AsO_2$, on the surface of the maghemite [154,156,159].

TEM and XRD measurements were conducted on both pure and As(V) adsorbed maghemites at pH 3 to eliminate the amorphous or crystal precipitation occurrence in the process (Paper II, Figure 6). From a visual observation of the TEM image, it was concluded that no amorphous precipitation had formed on the surface of the nanoparticles. Crystal precipitation was also excluded by a XRD patterns comparison.

As(V) adsorption onto maghemite nanoparticles was discovered to form an inner-sphere surface complex. An inner-sphere surface complex forms a monolayer onto the surface of an adsorbent, therefore the fit of experimental data to the Langmuir isotherm is in agreement with molecular scale investigations. Mechanochemical maghemite formed a bidentate binuclear complex, $(FeO)_2AsO_2$, with As(V) oxoanion at all studied pH values, while sol-gel and commercial maghemite only at pH 3. At pH values 5, 7, and 9, sol-gel and commercial maghemite formed a monodentate complex, $(FeO)AsO_3^-$ with arsenate. Several studies have also indicated an inner-sphere complex formation with As(V) adsorption onto different kinds of iron oxides [156,159] and even with maghemite nanoparticles [160].

4.5 Maghemite stability and regeneration

Stability of the maghemite nanoparticles were investigated by following iron dissolution with iron analysis in adsorbate solution after adsorption (Paper I) and regeneration experiments (Paper III). Iron was not detected after single adsorption experiments at pH values of 3, 5, 7, and 9 with mechanochemical, sol-gel, and commercial maghemites (Paper I). When studying the maghemite stability after regeneration experiments with sol-gel and commercial maghemite, it was observed that the iron dissolution during the cycling experiments was minimal for both adsorbents (Paper III). A maximum 0.5% of iron was dissolved with sol-gel and 0.1% with commercial maghemite from the total mass of adsorbent used. The iron content was measured after all successive experiments, from which dissolution was observed only after adsorption experiments at pH 3. (Desorption was conducted at pH> 12.)

Regeneration performed by 1 M NaOH showed ≥95% regeneration efficiencies for sol-gel and commercial maghemite when average values of As(V) adsorption capacity were used for efficiency calculations (Table 4.8).

Table 4.8. Regeneration of sol-gel and commercial maghemite for As(V) by 1 M NaOH.

Maghemite	**$C_{initial}$ As(V) (mg/L)**	**No. of cycles**	**Adsorption capacity of As(V), average value**		**RE[a] (%)**
			Before regeneration (mg/g)	**After regeneration (mg/g)**	
Sol-gel	0.5	6	4.8±0.1	4.6±0.7	96
	1.0	6	9.3±0.2	9.9±1.0	106
	3.0	6	17.8±0.8	17.0±0.9	96
Commercial	0.5	3	2.0±0.2	2.2±0.6	110
	1.0	3	3.7±0.01	3.5±0.3	95
	3.0	2	5.5±0.04	5.4±1.1	98

[a]RE = Regeneration Efficiency

When comparing the separate results within each cycle, the same efficiencies (≥95%) were observed with commercial maghemite with all initial As(V) concentrations and 0.5 and 1 mg As(V)/L with sol-gel maghemite, while over 90% of its adsorption capacity was restored at an As(V) initial concentration of 3 mg/L (Paper III, Figures 5 and 6). With such high regeneration efficiencies, it can be concluded that arsenate adsorption/desorption is a reversible process, even though arsenate is attached to maghemite with a strong bond forming an inner-sphere surface complex. Sol-gel maghemite performed two to three times more regeneration cycles than commercial maghemite. The reason for the poor

cycle performance of commercial maghemite is the heavy loss of the adsorbent during experiments and the filtering process, leading to a smaller amount of adsorbent mass and too little desorption solution volume to continue cycling tests further with a reliable outcome. Commercial maghemite disperses more in water than sol-gel maghemite and is therefore more difficult to operate.

5. CONCLUSIONS

Maghemite nanoparticles were successfully synthesized by sol-gel and mechanochemical methods, with the sol-gel method being faster and more convenient to work with. The characterization of all three different kinds of maghemites revealed that mechanochemical maghemite possesses the smallest particle size (3.8 nm) of the studied magnetic nanoparticles, followed by sol-gel (12.1 nm) and commercial maghemite (18.4 nm). All maghemite particles had a crystalline phase and the cubic structure of maghemite. However, the crystal packing varied from well-ordered (commercial) to disordered (mechanochemical), which was observable in the FTIR spectra and XRD pattern. The particle size was found to have an influence on magnetic properties and the specific surface area of maghemites: the smaller the particle, the higher the specific surface area and the weaker the magnetization value. None of the studied maghemites possessed the quality of a hard magnet.

Adsorption equilibrium was reached in the same timeframe of 30-50 hours for all maghemites, and the kinetics followed the typical behaviour of heavy metal adsorption onto an oxide surface. The first rapid stage of kinetics is presumably the fast external diffusion followed by a slower reaction stage, which is caused by inner-sphere complex formation. Such a complex formation was indicated by fitting the kinetics data to a pseudo-second order kinetic model, resulting in a high correlation coefficient value and molecular scale investigations. During the rapid stage (approx. 30 min), 70-90% of arsenate was adsorbed onto the maghemites, with commercial maghemite showing the highest removal efficiency, followed by sol-gel and mechanochemical maghemite. Arsenate desorption was conducted by 1 M NaOH and desorption kinetics also obeyed a pseudo-second order kinetic model. The magnetic separation of maghemites with a hard magnet was most favourable with sol-gel maghemite.

Experimental data of all maghemites fit well with the Langmuir isotherm, and it was observed that all three maghemites adsorb arsenate with

reasonable capacity. The maximum adsorption capacity was the highest at pH 3 for all maghemites. Mechanochemical maghemite achieved the highest adsorption capacity among these three adsorbents, 50.0 mg/g, while adsorption capacities for sol-gel and commercial maghemite were 25.0 mg/g and 16.7 mg/g, respectively. The difference in capacities is due to the specific surface area of the nanoparticles and a pH effect. Arsenate adsorption capacity was affected by competing ions, such as phosphate (PO_4-P) and silicate (SiO_2), when examining the effect with initial As(V) concentrations of 0.5, 1.0, and 3.0 mg/L. A phosphate (0.5 , 1.5, and 2.9 mg/L) effect was significant both at pH 3 and 7 and silicate (10, 30, and 50 mg/L) at pH 7. The sulphate (20 and 250 mg/L) and nitrate (1 and 12 mg/L) competing effect was insignificant at pH 3. The removal of arsenate (0.5 mg As(V)/L) from the groundwater sample was as efficient as from laboratory water, both at pH 3 and pH 7.

A molecular-scale investigation of the adsorption mechanism revealed that arsenate forms an inner-sphere surface complex onto iron oxide surface. At all studied pH values, mechanochemical maghemite formed bidentate binuclear complex with arsenate, $(FeO)_2AsO_2$, while sol-gel and commercial maghemite at only pH 3. Arsenate formed a monodentate complex, $(FeO)AsO_3$, with sol-gel and commercial maghemite at pH values of 5, 7, and 9.

Even though arsenate forms such a strong bond with maghemite, it was observed that adsorption/desorption is a reversible process. Chemical regeneration of maghemite was conducted by 1 M NaOH and concentrations of 0.5, 1 and 3 mg As(V)/L, sol-gel maghemite showing a longer cycling capability (6 cycles) than commercial maghemite (2-3 cycles). More than 95% of the initial uptake capacity was maintained with both maghemites. Maghemite stability was studied by observing the iron dissolution during the regeneration experiments, and it was detected to be minimal for both maghemites. A maximum 0.5% of iron was dissolved with sol-gel and 0.1% with commercial maghemite from the total mass of adsorbent used.

When the physical and adsorptive properties of three studied maghemites were compared, sol-gel maghemite proved to be the most suitable one for future studies. This is because sol-gel synthesis is convenient, fast, and repeatedly produces high quality particles. Sol-gel maghemite adsorbs arsenate satisfactorily, and there is no need for preliminary treatment(s) prior to adsorption experiments. It is convenient to handle and separate via

an external magnet. Moreover, sol-gel maghemite maintains its initial arsenate adsorption capacity after six regeneration cycles and is stable, which are important factors for cost-effectiveness. Among studied maghemites, mechanochemical maghemite showed the highest arsenate adsorption capacity at pH 3 (50 mg/g). However, its demanding synthesis post-treatment and weak magnetic properties do not support continuing adsorption studies with it. Commercial maghemite showed the lowest arsenate adsorption capacity and was the most difficult to operate.

Activated alumina is the most common adsorbent used for arsenic removal. Compared to its properties over sol-gel maghemite, a couple of similarities can be addressed. Both of them require pH control, interfere with other ions, and can be regenerated by alkaline solution, thus needing careful monitoring. Adsorption capacities can meet the same level, but in general, activated alumina can remove slightly more arsenate than sol-gel maghemite. In other properties, such as the simple and rapid separation via external magnet, waste formation, and adsorbent stability, sol-gel maghemite overcomes activated alumina. In the case of sol-gel maghemite, the dose (mass/volume ratio) needed to remove 0.5 mg/L of arsenate to the WHO guideline level (<0.010 mg/L) is 0.1 g/L. Thus, for example, if 20 litres of water were purified daily, it would produce only 730 g of "arsenate-maghemite" waste in a year. Accordingly, waste formation with activated alumina would be 7.3 kg (dose 1 g/L), or even higher, due to dissolution of activated alumina. Based on the aforementioned facts, it can be concluded that sol-gel maghemite is able to compete with activated alumina for adsorbent properties.

This laboratory-scale research pointed out the suitability of sol-gel maghemite for arsenate removal by adsorption. These research results can be used as ground information for subsequent research in which sol-gel maghemite will be employed in the pilot/full-scale applications. Future studies with sol-gel maghemite should focus on four areas: (1) synthesis, (2) further adsorption studies focusing on the pilot/full-scale applications, (3) arsenate-maghemite/ maghemite nanoparticles waste handling, and (4) development of magnetic separation. When sol-gel maghemite is used in industrial applications, more than a few grams are needed, so its synthesis should be developed so that mass production is possible. Adsorption studies should be conducted with natural water samples and with POU or pilot scale as well as on the waterworks level, for example with fixed bed adsorption systems. It would also be useful to study the performance of the maghemites in removal of arsenite species from the water. The waste

handling of arsenate containing nanoparticles should be carefully investigated, since this of financial interest not only to water works plants but also to environmental officials. For magnetic separation with HGMC, it would be interesting to conduct experiments both batch and continuous flow processes. Consequently, research still needs to be done with maghemite nanoparticles to gather relevant information for their use in a POU/full-scale application and to gain the position of a widely used nanoadsorbent for arsenic removal. The fundamental research presented in this thesis was the first step in paving the way to the use of maghemite nanoparticles for arsenic removal from drinking water – a global challenge concerning over a billion people.

References

[1] WHO, *Guidelines for drinking water quality 1*, 2006.

[2] M. Bissen, F.H. Frimmel, Arsenic- a review. Part II: oxidation of arsenic and its removal in water treatment, *Acta hydrochim. hydrobiol.* 31 (2003) 97-107.

[3] D. Mohan, C.U. Pittman Jr., Arsenic removal from water/wastewater using adsorbents – a critical review, *J. Hazard. Mater.* 142 (2007) 1-53.

[4] S.R. Kanel, J.-M. Greneche, H. Choi, Arsenic(V) removal from groundwater using nano scale zero-valent iron as a colloidal reactive barrier material, *Environ. Sci. Technol.* 40 (2006) 2045-2050.

[5] M.E. Pena, G.P. Korfiatis, M. Patel, L. Lippincott, X. Meng, Adsorption of As(V) and As(III) by nanocrystalline titanium dioxide, *Water Res.* 39 (2005) 2327-2337.

[6] S. Yean, L. Cong, C.T. Yavuz, J.T. Mayo, W.W. Yu, A.T. Kan, V.L. Colvin, M.B. Tomson, Effect of magnetite particle size on adsorption and desorption of arsenite and arsenate, *J. Mater. Res.* 20 (2005) 3255-3264.

[7] M. Köhler, W. Fritzsche, *Nanotechnology – an introduction to nanostructuring techniques*, Wiley, Weinheim, 2004.

[8] R.J. Aitken, M.Q. Chaudhry, A.B.A. Boxall, M. Hull, Manufacture and use of nanomaterials: current status in the UK and global trends, *Occup. Med.* 56 (2006) 300-306.

[9] M. Wilson, K. Kannangara, G. Smith, M. Simmons, B, Raguse, *Nanotechnology – basic science and emerging technologies*, CRC, Boca Raton, 2002.

[10] L. Theodore, R.G. Kunz, *Nanotechnology: environmental implications and solutions*, Wiley, New Jersey, 2005.

[11] N. Savage, M. Diallo, J. Duncan, A. Street, R. Sustich, *Nanotechnology applications for clean water*, William Andrew, NY, USA, 2009.

[12] D.G. Rickerby, M. Morrison, Nanotechnology and the environment: A European perspective, *STAM* 8 (2007) 19-24.

[13] N. Savage, M.S. Diallo, Nanomaterials and water purification: opportunities and challenges, *J. Nanopart. Res.* 7 (2005) 331-342.

[14] Y.C. Sharma, V. Srivastava, V.K. Singh, S.N. Kaul, C.H. Weng, Nano-adsorbents for the removal of metallic pollutants form water and wastewater, *Environ. Technol.* 30 (2009) 583-609.

[15] J. Hu, G. Chen, I.M.C. Lo, Removal and recovery of Cr(VI) from wastewater by maghemite nanoparticles, *Water Res.* 39 (2005) 4528-4536.

[16] R.S. Oremland, J.F. Stolz, The ecology of arsenic, *Science* 300 (2003) 939-944.

[17] P.L. Smedley, D.G. Kinniburgh, A review of the source, behaviour and distribution of arsenic in natural waters, *Appl. Geochem.* 17 (2002) 517-568.

[18] C.K. Jain, I. Ali, Arsenic: occurrence, toxicity and speciation techniques, *Water Res.* 34 (2000) 4304-4312.

[19] B. Backman, P. Lahermo, *Arsenic in groundwater. Arsenic in Finland: Distribution, Environmental Impacts and Risks*, Geological Survey of Finland, 2004.

[20] D. Chakraborti, M.M. Rahman, K. Paul, U.K. Chowdhury, M.K. Sengupta, D. Lodh, C.R. Chanda, K.C. Saha, S.C. Mukherjee, Arsenic calamity in the Indian subcontinent. What lessons have been learned? *Talanta* 58 (2002) 3-22.

[21] S.-L. Chen, S.R. Dzeng, M.-H. Yang, Arsenic species in groundwaters of the blackfoot disease area, Taiwan, *Environ. Sci. Technol.* 28 (1994) 877-881.

[22] M. Karim, Arsenic in groundwater and health problems in Bangladesh, *Water. Res*. 34 (2000) 304-310.

[23] European Commission Directive. *98/83/EC, related with drinking water quality intended for human consumption*, Brussels, Belgium, 1998.

[24] USEPA, *Federal register* 68, 14501-14507, 2003.

[25] P. Mondal, C.B. Majumder, B. Mohanty, Laboratory based approaches for arsenic remediation from contaminated water: recent developments, *J. Hazard. Mater*. B137 (2006) 464-479.

[26] X.-P. Yan, R. Kerrich, M.J. Hendry, Distribution of arsenic(III), arsenic(V) and total inorganic arsenic in porewaters form a thick till and clay-rich aquitard sequence, Saskatchewan, Canada, *Geochim. Cosmochim. Acta* 64 (2000) 2637-2648.

[27] P.K. Dutta, S.O. Pehkonen, V.K. Sharma, A.K. Ray, Photocatalytic oxidation of arsenic(III): evidence of hydroxyl radicals, *Environ. Sci. Technol*. 39 (2005) 1827-1834.

[28] M. Zaw, M.T. Emett, Arsenic removal from water using advanced oxidation processes, *Toxicol. Lett*. 133 (2002) 113-118.

[29] USEPA, *Arsenic treatment technologies for soil, waste and water*, EPA-542-R-02-004, 2002.

[30] Y. Salameh, N. Al-Lagtah, M.N.M. Ahmad, S.J. Allen, G.M. Walker, Kinetic and thermodynamic investigations on arsenic adsorption onto dolomitic sorbents, *Chem. Eng. J*. 160 (2010) 440-446.

[31] G.Gerente, Y. Andres, G. McKay, P. Le Cloirec, Removal of arsenic(V) onto chitosan: from sorption mechanism explanation to dynamic water treatment process, *Chem. Eng. J*. 158 (2010) 593-598.

[32] J.R. Parga, D.L. Cocke, J.L. Valenzuela, J.A. Gomes, M. Kesmez, G. Irwin, H. Moreno, M. Weir, Arsenic removal via electrocoagulation from heavy metal contaminated groundwater in La Comarc Lagunera Mexico, *J. Hazard. Mater*. B124 (2005) 247-254.

[33] L. Feenstra, J. van Erkel, L. Vasak, *Arsenic in groundwater: Overview and evaluation of removal methods*, Report nr. SP 2007-2, International Groundwater Resources Assessment Centre (IGRAC), 2007.

[34] M. Leist, R.J. Casey, D. Caridi, The management of arsenic wastes: problems and prospects, *J. Hazard. Mater.* B76 (2000) 125-138.

[35] D.L. Sparks, *Environmental Soil Chemistry*, second ed., Academic press, San Diego, California, 2003.

[36] G. Sposito, On points of zero charge, *Environ. Sci. Technol.* 32 (1998) 2815-2819.

[37] D. Basmadjian, *The little adsorption book*, CRC Press, Boca Raton 1997.

[38] F.L. Slejko, *Adsorption technology*, CRC, New York, 1985.

[39] A.Dabrowski, Adsorption – from theory to practice, *Adv. Colloid Interface Sci.* 93 (2001) 135-224.

[40] M.M. Benjamin, *Water chemistry*, McGraw Hill, Singapore 2002.

[41] S. J. Allen, G. McKay, J.F. Porter, Adsorption isotherm models for basic dye adsorption by peat in single and binary component systems, *J. Colloid Interface Sci.* 280 (2004) 322-333.

[42] G. Limousin, J.-P. Gaudet, L. Charlet, S. Szenknect, V. Barthes, M. Krimissa, Sorption isotherms: a review on physical bases, modeling and measurement, *Appl. Geochem.* 22 (2007) 249-275.

[43] A. Jain, R.H. Loeppert, Effect of competing anions on the adsorption of arsenate and arsenite by ferrihydrite, *J. Environ. Qual.* 29 (2000) 1422-1430.

[44] T. Möller, P. Sylvester, Effect of silica and pH on arsenic uptake by resin/iron oxide hybrid material, *Wat. Res.* 42 (2008) 1760-1766.

[45] M. Grafe, M.J. Eick, P.R. Grossl, A.M. Saunders, Adsorption of arsenate and arsenite on ferrihydrite in the presence and absence of dissolved organic carbon, *J. Environ. Qual.* 31 (2002) 1115-1123.

[46] T.P. Luxton, M.J. Eick, D.J. Rimstidt, The role of silicate in the adsorption/desorption of arsenite on goethite, *Chem. Geol.* 252 (2008) 125-135.

[47] F. Rubel Jr., EPA/600/R-03/019, *Design manual: removal of arsenic from drinking water by adsorptive media*, US EPA, 2003.

[48] G.D. Moeser, K.A. Roach, W.H. Green, T.A. Hatton, P.E. Laibinis, High-gradient magnetic separation of coated magnetic nanoparticles, *A.I.Ch.E. Journal,* 50 (2004) 2835-2848.

[49] C.T. Yavuz, A. Prakash, J.T. Mayo, V.L. Colvin, Magnetic separations: from steel plants to biotechnology, *Chem. Eng. Sci.* 64 (2009) 2510-2521.

[50] T. Uslu, U. Atalay, A.I. Arol, Effect of microwave heating on magnetic separation of pyrite, *Colloids. Surf. A* 225 (2003) 161-167.

[51] J. Iannicelli, J. Pechin, Magnetic separation of kaolin clay using an advanced 9 T separator, *IEEE Trans. Appl. Supercond.* 10 (2000) 917-922.

[52] A.D. Ebner, J.A. Ritter, J.D. Navratil, Adsorption of cesium, strontium, and cobalt ions on magnetite and a magnetite-silica composite, *Ind. Eng. Chem. Res.* 40 (2001) 1615-1623.

[53] I. Safarik, K. Nymburska, M. Safarikova, Adsorption of water-soluble organic dyes on magnetic charchoal, *J. Chem. Technol. Biotechnol.* 69 (1997) 1-4.

[54] I. Safarik, M. Safarikova, Magnetic nanoparticles and biosciences, *M. Fur Chem.* 133 (2002) 737-759.

[55] R. Ambashta, M. Sillanpää, Water purification using magnetic assistance: a review, *J. Hazard. Mat.* 180 (2010) 38-49.

[56] R.M. Wingo, D.J. Devlin, D.D. Hill, D.D. Padilla, F.C. Pregner, L.A. Worl, Capture and retrieval of plutonium oxide particles at ultra-low concentrations using high-gradient magnetic separation, *Sep. Sci. Technol.* 37 (2002) 3715-3726.

[57] I.Ihara, K. Kanamura, E. Shimada,T. Watanabe, High gradient magnetic separation combined with electrocoagulation and electrochemical oxidationfor the treatment of landfill leachate, *IEEE Trans. Appl. Supercond.* 14 (2004) 1558-1560.

[58] H. Isogami, S. Miyabayashi, M. Morita, *Magnetic separation apparatus and waste water treatment apparatus*, US Patent 20110215041A1 Sep. 8, 2011.

[59] S. Nishijima, S. Takeda, Research and development of super-conducting high gradient magnetic separation for purification of wastewater from paper factory, *IEEE Trans. Appl. Supercond.* 17 (2007) 2311-2314.

[60] T.H. Boyer, P.C. Singer, Bench-scale testing of a magnetic ion exchange resin for removal of disinfection by-product precursors, *Wat. Res.* 39 (2005) 1265-1276.

[61] A.K. Jha, A. Bose, J.P. Downey, Removal of As(V) and Cr(VI) ions from aqueous solution using a continuous, hybrid field-gradient magnetic separation device, *Sep. Sci. Technol.* 41 (2006) 3297-3312.

[62] A.Nowack, T.D. Bucheli, Occurrence, behavior and effects of nanoparticles in the environment, *Environ. Pollut.* 150 (2007) 5-22.

[63] S.P. Gubin, Y.A. Koksharov, G.B. Khomutov, G.Y. Yrukov, Magnetic nanoparticles: preparation, structure and properties, *Russian Chem. Rev.* 74 (2005) 489-520.

[64] F. Fendrych, L. Kraus, O. Chayka, P. Lobotka, I. Vavra, J. Tous, V. Studnicka, Z. Frait, Preparation of nanostructured magnetic films by the plasma jet technique, *Monatsh. Chem.* 133 (2002) 773-784.

[65] X.G. Li, A. Chiba, S. Takahashi, K. Ohsaki, Preparation, oxidation and magnetic properties of Fe-Cr ultrafine powders by hydrogen plasma-metal reaction, *J. Magn. Magn. Mater.* 173 (1997) 101-108.

[66] B. Martinez, A. Roig, X. Obradors, E. Molins, A. Rouanet, C. Monty, Magnetic properties of γ-Fe_2O_3 nanoparticles obtained by vaporization condensation in a solar furnace, *J. Appl. Phys.* 79 (1996) 2580-2586.

[67] A. Tavakoli, M. Sohrabi, A. Kargari, A review of methods for synthesis of nanostructured metals with emphasis on iron compounds, *Chem. Pap.* 61 (2007) 151-170.

[68] P.G. McCormick, T. Tsuzuki, J.S. Robinson, J. Ding, Nanopowders synthesized by mechanochemical processing, *Adv. Mater.* 13 (2001) 1008-1010.

[69] T. Tsuzuki, P.G. McCormick, Mechanochemical synthesis of nanoparticles, *J. Mater. Sci.* 39 (2004) 5143-5146.

[70] B.L. Cushing, V.L. Kolesnichenko, C.J. O'Connor, Recent advances in the liquid-phase syntheses of inorganic nanoparticles, *Chem. Rev.* 104 (2004) 3893-3946.

[71] Y.Lu, Y.Yin, B.T. Mayers, Y. Xia, Modifying the surface properties of superparamagnetic iron oxide nanoparticles through a sol-gel approach, *Nano Lett.* 2 (2002) 183-186.

[72] T. Prozorov, G. Kataby, R. Prozorov, A. Gedanken, Effect of surfactant concentration on the size of coated ferromagnetic nanoparticles, *Thin Solid Films* 340 (1999) 189-193.

[73] L. Theodore, *Nanotechnology – basic calculations for engineers and scientists*, Wiley, New Jersey, 2006.

[74] Y.U. Akimov, Fields of application of aerogels (Review), *Instrum. Experim. Techn.* 46 (2003) 287-299.

[75] Z. Chen, L. Gu, The sol-gel transition of mullite spinning solution in relation to the formation of ceramic fibers, *J. Sol-Gel Sci. Technol.* 46 (2008) 23-32.

[76] A.Conde, J. de Damborenea, A. Duran, M. Menning, Protective properties of a sol-gel coating on zinc coated steel, *J. Sol-Gel Sci. Technol.* 37 (2006) 79-85.

[77] S. Sakka, H. Kozuka, Sol-gel preparation of coating films containing noble metal colloids, *J. Sol-Gel Sci. Technol.* 13 (1998) 701-705.

[78] O.A. Shilova, S. V. Hashkovsky, L.A. Kuznetsova, Sol-gel preparation of ceramic coating for electrical, laser, space engineering and power, *J. Sol-Gel Sci. Technol.* 26 (2003) 687-691.

[79] T.C. Zhang, R.Y. Surampalli, K.C.K. Lai, Z. Hu, R.D. Tyngi, I.M.C. Lo, *Nanotechnologies for water environment applications*, ASCE, Virginia, 2009.

[80] H. Schmidt, Nanoparticles by chemical synthesis, processing to materials and innovative applications, *Appl. Organom. Chem.* 15 (2001) 331-343.

[81] A.-H. Lu, E.L. Salabas, F. Schüth, Magnetic nanoparticles: synthesis, protection, functionalization, and application, *Angew. Chem. Int. Ed.* 46 (2007) 1222-1244.

[82] U. Schwertmann, R.M. Cornell, *The iron oxides: structure, properties, reactions, occurrence and uses*, second ed., Wiley-VCH, Weinheim, 2000.

[83] A. Bianco, M. Prato, Can carbon nanotubes be considered useful tools for biological applications? *Adv. Mater.* 15 (2003) 1765-1768.

[84] K.K. Jain, The role of nanobiotechnology in drug discovery, *Drug Discov. Today* 10 (2005) 1435-1442.

[85] S.J. Son, X. Bai, S.B. Lee, Inorganic hollow nanoparticles and nanotubes in nanomedicine. Part 2: imaging, diagnostic and therapeutic applications, *Drug Discov. Today* 12 (2007) 657-663.

[86] M. Brust, C.J. Kiely, Some recent advances in nanostructure preparation from gold and silver particles: a short topical review, *Colloids. Surf. A* 202 (2002) 175-186.

[87] S. Guo, E. Wang, Synthesis and electrochemical applications of gold nanoparticles, *Anal. Chim. Acta* 598 (2007) 181-192.

[88] W.-T. Liu, Nanoparticles and their biological and environmental applications, *J. Biosci. Bioeng.* 102 (2006) 1-7.

[89] W.-X. Zhang, Nanoscale iron particles for environmental remediation: an overview, *J. Nanopart. Res.* 5 (2003) 323-332.

[90] A.K. Gupta, M. Gupta, Synthesis and surface engineering of iron oxide nanoparticles for biomedical applications, *Biomaterials* 26 (2005) 3995-4021.

[91] J. Lu, S. Yang, K.M. Ng, C.-H. Su, C.-S. Yeh, Y.-N. Wu, D.-B. Shieh, Solid-state synthesis of monocrystalline iron oxide particle based ferrofluid suitable for magnetic resonance imaging contrast application, *Nanotech.* 17 (2006) 5812-5820.

[92] A.Favre-Reguillon, G.Lebuzit, J. Fooz, A. Guy, Selective concentration of uranium from seawater by nanofiltration, *Ind. Eng. Chem. Res.* 42 (2003) 5900-5904.

[93] B. Van der Bruggen, C. Vandecasteele, Removal of pollutants from surface water and groundwater by nanofiltration: overview of possible applications in the drinking water industry, *Environ. Pollut.* 122 (2003) 435-445.

[94] M.S. Mohsen, J.O. Jaber, M.D. Afonso, Desalination of brakish water by nanofiltration and reverse osmosis, *Desalination* 157 (2003) 167-167.

[95] F.M. Koehler, M. Rossier, M. Waelle, E.K. Athanassiou, L.K. Limbach, R.N.Grass, D. Guenther, W.J. Stark, Magnetic EDTA: coupling heavy metal chelators to metal nanomagnets for rapid removal of cadmium, lead and copper from contaminated water, *Chem. Commun.* (2009) 4862-4864.

[96] K. Kabra, R. Chaudhary, R. L. Sawhney, Treatment of hazardous organic and inorganic compounds through aqueous-phase photocatalysis: A review, *Ind. Eng. Chem. Res.* 43 (2004) 7683-7696.

[97] J. T. Nurmi, P.G. Tratnyek, V. Sarathy, D.R. Baer, J. E. Amonette, K. Pecher, C. Wang, J.C. Linehan, D. W. Matson, R.L. Penn, M.D. Driessen, Characterization and properties of metallic iron nanoparticles: spectroscopy, electrochemistry and kinetics, *Environ. Sci. Technol.* 39 (2005) 1221-1230.

[98] X. Cheng, A.T. Kan, M.B. Tomson, Naphthalene adsorption and desorption from aqueous C_{60} fullerene, *J. Chem. Eng. Data* 49 (2004) 675-683.

[99] C.L. Mangun, Z.R. Yue, J. Economy, S. Maloney, P. Kemme, D. Cropek, Adsorption of organic contaminants from water using tailored ACFs carbon, *Chem. Mater.* 13 (2001) 2356-2360.

[100] X.J. Peng, Y.H. Li, Z.K. Luan, Z.C. Di, H.Y. Wang, B.H. Tian, Z.P. Jia, Adsorption of 1,2-dichlorobenzene from water to carbon nanotubes, *Chem. Phys. Lett.* 376 (2003) 154-158.

[101] I.Sondi, B. Salopek-Sondi, Silver nanoparticles as antimicrobial agent: a case study of *E-coli* as a model for gram-negative bacteria, *J. Coll. Interf. Sci.* 275 (2004) 177-182.

[102] P.K. Stoimenov, R.L. Klinger, G.L. Marchin, K.J. Klabunde, Metal oxide nanoparticles as bactericidal agents, *Langmuir* 18 (2002) 6679-6686.

[103] S.S. Banerjee, D.-H. Chen, Fast removal of copper ions by gum Arabic modified magnetic nano-adsorbent, *J. Hazard. Mat.* 147 (2007) 792-799.

[104] J. Hu, I.M.C. Lo, G. Chen, Removal of Cr(VI) by magnetite nanoparticles, *Water Sci. Tech.* 50 (2004) 139- 146.

[105] J. Hu, I.M.C. Lo, G. Chen, Fast removal and recovery of Cr(VI) using surface-modified jacobsite ($MnFe_2O_4$) nanoparticles, *Langmuir* 21 (2005) 11173-11179.

[106] J. Hu, G. Chen, I.M.C. Lo, Selective removal of heavy metals form industrial wastewater using maghemite nanoparticle: performance and mechanism, *J. Env. Eng.* 132 (2006) 709-715.

[107] J. Hu, I.M.C. Lo, G. Chen, Performance and mechanism of chromate (VI) adsorption by δ-FeOOH-coated maghemite (γ-Fe_2O_3) nanoparticles, *Sep. Purif. Technol.* 58 (2007) 76-82.

[108] J. Hu, I.M.C. Lo, G. Chen, Comparative study of various magnetic nanoparticles for Cr(VI) removal, *Sep. Purif. Technol.* 56 (2007) 249-256.

[109] Y. Kim, B. Lee, J. Yi, Preparation of functionalized mesostructured silica containing magnetite (MSM) for the removal of copper ions in aqueous solutions and its magnetic separation, *Sep. Sci. Techn.* 38 (2003) 2533-2548.

[110] A.-F. Ngomsik, A. Bee, J.-M. Siaugue, V. Cabuil, G. Cote, Nickel adsorption by magnetic alginate microcapsules containing an extractant, *Wat. Res.* 40 (2006) 1848-1856.

[111] Y.-C. Chang, S.-W. Chang, D.-H. Chen, Magnetic chitosan nanoparticles: studies on chitosan binding and adsorption of Co(II) ions, *React. Funct. Polym.* 66 (2006) 335-341.

[112] Meridian Institute, *Background paper for the international workshop on nanotechnology, water, and development, Conventional water treatment technologies, nano-based treatment technologies*, Chennai, 2006.

[113] P.K. Dutta, A.K. Ray, V.K. Sharma, F.J. Millero, Adsorption of arsenate and arsenite on titanium dioxide suspensions, *J. Colloid Interface Sci.* 278 (2004) 270-275.

[114] M.A.Ferguson, M.R. Hoffman, J.G. Hering, TiO_2-photocatalyzed As(III) oxidation in aqueous suspensions: reaction kinetics and effects on adsorption, *Environ. Sci. Technol.* 39 (2005) 1880-1886.

[115] K. Hristovski, A. Baumgardner, P. Westerhoff, Selecting metal oxide nanomaterials for arsenic removal in fixed bed columns: from nanopowders to aggregated nanoparticle media, *J. Haz. Mat.* 147 (2007) 265-274.

[116] E. A. Deliyanni, D.N. Bakoyannakis, A.I. Zouboulis, K.A. Matis, Sorption of As(V) ions by akaganéite-type nanocrystals, *Chemosphere* 50 (2003) 155-163.

[117] O.M. Vatutsina, V.S. Soldatov, V.I. Sokolova, J. Johann, M. Bissen, A. Weissenbacher, A new hybrid (polymer/inorganic) fibrous sorbent for arsenic removal from drinking water, *React. Funct. Polym.* 67 (2007) 184-201.

[118] G. Jegadeesan, K. Mondal, S.B. Lalvani, Arsenate remediation using nanosized modified zerovalent iron particles, *Env. Prog.* 24 (2005) 289-296.

[119] J.T. Mayo, C. Yavuz, S. Yean, L. Cong, H. Shipley, W. Yu, J. Falkner, A. Kan, M. Tomson, V.L. Colvin, The effect of nanocrystalline magnetite size on arsenic removal, *Sci. and Tech. of Adv. Mat.* 8 (2007) 71-75.

[120] J.G. Parsons, M.L. Lopez, J.R. Peralta-Videa, J.L. Gardea-Torresdey, Determination of arsenic(III) and arsenic(V) binding to microwave assisted hydrothermal synthetically prepared Fe_3O_4, Mn_3O_4 and $MnFe_2O_4$ nanoadsorbents, *Microchem J.* 91 (2009) 100-106.

[121] T. Turk, I. Alp, H. Deveci, Adsorption of As(V) from water using nanomagnetite, *J. Env. Eng.* 136 (2010) 399-404.

[122] H. Park, N.V. Myung, H. Jung, H. Choi, As(V) remediation using electrochemically synthesized maghemite nanoparticles, *J. Nanopart. Res.* 11 (2009) 1981-1989.

[123] W.W.Yu, J.C. Falkner, C.T. Yavuz, V.L. Colvin, Synthesis of monodisperse iron oxide nanocrystals by thermal decomposition of iron carboxylate salts, *Chem. Commun.* 20 (2004) 2306-2307.

[124] C.H. Cooper, A.G. Cummins, M.Y. Starostin, C.P. Honsinger, *Nanomesh article and method of using the same for purifying fluids*, United States Patent Application 20050263456, December 1, 2005.

[125] S.R.Yoon, S.S. Kim, H. Hyung, Y.H. Kim, *Domestic nanofiltration membrane based water purifier without storage tank*, US Patent 6841068 January 11, 2005.

[126] T. Hillie, M. Munasinghe, M. Hlope, Y. Deraniyagala, *Nano-technology, water & development*, Meridian Institute, 2006.

[127] E. E. Koslow, *Microporous filter media, filteration systems containing same, and methods of making and using*, US Patent 6913154, June 5, 2005.

[128] G.E. Fryxell, J. Liu, T.A.Hauser, Z. Nie, K.F. Ferris, S. Mattigold, M. Gong, R.T. Hallen, Design and synthesis of selective mesoporous anion traps, *Chem. Mater.* 11 (1999) 2148-2154.

[129] S.D. Kelly, K.M. Kemner, G.E. Fryxell, J. Liu, S.V. Mattigod, K.F. Ferris, X-ray-adsorption fine-structure spectroscopy study of the interactions between contaminant tetrahedral anions and self-assembled monolayers on mesoporous supports, *J. Phys.Chem. B* 105 (2001) 6337-6346.

[130] P. Sylvester, P. Westerhoff, T. Möller, M. Badruzzaman, O. Boyd, A hybrid sorbent utilizing nanoparticles of hydrous iron oxide for arsenic removal from drinking water, *Env. Eng. Sci.* 24 (2007) 104-112.

[131] A.S.C.Chen, L. Wang, J.L. Oxenham, W.E. Condit, 2004. *Capital costs of arsenic removal technologies*, *U.S. EPA arsenic removal technologies demonstration program round 1*. EPA 68-C-00-185, 2004.

[132] E.K. Athanassiou, R.N. Grass, Magnetic recovery of toxic heavy metals for water purification process, *Env. Nano Technol.* 2 (2010) 40-43.

[133] Bayoxide E33 Fact Sheet, http://www.adedgetech.com/pdfs/litpdfs/E33%20literature/E33_MEDIA_0309.pdf

[134] F.W.Vance, Dealing with “nearly perfect” water- unintended consequenses of arsenic removal, *Water Cond. & Purif.* Jan (2010) 13-14.

[135] S. Veintemillas-Verdaguer, M.P. Morals, C.J. Serna, Continuous production of γ-Fe_2O_3 ultrafine powders by laser pyrolysis, *Mater. Lett.* 35 (1998) 227-231.

[136] S. Yu, G.M. Chow, Carboxyl group (-CO_2H) functionalized ferromagnetic iron oxide nanoparticles for potential bio-applications, *J. Mater. Chem.* 14 (2004) 2781-2786.

[137] Y. Jeong, F. Maohong, J. Van Leeuwen, J.F. Belczyk, Effect of competing solutes on arsenic(V) adsorption using iron and aluminium oxides, *J. Environ. Sci.* 19 (2007) 910-919.

[138] C.-R. Lin, Y.-M. Chu, S.-C. Wang, Magnetic properties of magnetite nanoparticles prepared by mechanochemical reaction, *Mater. Let.* 60 (2006) 447-450.

[139] Colloidal Dynamics Pty Ltd., Electroacoustics *tutorials, zeta potential, colloidal dynamics leaders in colloid measurement*, Australia, 1999.

[140] A.M. Scheidegger, G.M. Lamble, D.L. Sparks, Spectroscopic evidence for the formation of mixed-cation hydroxide phases upon metal sorption on clays and aluminum oxides, *J. Colloid Interface Sci.* 186 (1997) 118-128.

[141] Y.S. Ho and G. McKay, Pseudo-second order model for sorption process, *Process Biochem.* 34 (1999) 451-465.

[142] M. Özacar, I.A. Sengil, H. Türkmenler, Equilibrium and kinetic data, and adsorption mechanism for adsorption of lead onto valonia tannin resin, *Chem. Eng. J.* 143 (2008) 32-42.

[143] K.P. Raven, A. Jain, R.H. Loeppert, Arsenite and arsenate adsorption on ferrihydrite: kinetics, equilibrium, and adsorption, *Environ. Sci. Technol.* 32 (1998) 344-349.

[144] T.-F. Lin, J.-K. Wu, Adsorption of arsenite and arsenate within activated alumina grains: equilibrium and kinetics, *Wat. Res.* 35 (2001) 2049-2057.

[145] Y. Kim, C. Kim, I. Choi, S. Rengaraj, Y. Yi, Arsenic removal using mesoporous alumina prepared via a templating method, *Environ. Sci. Technol.* 38 (2004) 924-931.

[146] D.B. Singh, G. Prasad, D.C. Rupainwar, Adsorption technique for the treatment of As(V)-rich effluents, *Colloid Surf. A* 111 (1996) 49-56.

[147] V. Lenoble, O. Bouras, V. Deluchat, B. Serpaud, J.-C. Bollinger, Arsenic adsorption onto pillared clays and iron oxides, *J. Colloid Interface. Sci.* 255 (2002) 52-58.

[148] J. A. Wilkie, J.G. Hering, Adsorption of arsenic onto hydrous ferric oxide: effects of adsorbate/adsorbent ratios and co-occurring solutes, *Colloid Surface A*, 107 (1996) 97-110.

[149] C.C. Davis, H.-W. Chen, M. Edwards, Modeling silica sorption to iron hydroxide, *Environ. Sci. Technol.* 36 (2002) 582-587.

[150] E. Smith, R. Naidu, A.M. Alston, Chemistry of inorganic arsenic in soils: II. Effect of phosphorus, sodium and calcium on arsenic sorption, *J. Environ. Qual.* 31 (2002) 557-563.

[151] A.D. Redman, D.L. Macalady, D. Ahmann, Natural organic matter affects arsenic speciation and sorption onto hematite, *Environ. Sci. Technol.* 36 (2002) 2889-2896.

[152] X. Meng, S. Bang, G.P. Korfiatis, Effects of silicate, sulfate and carbonate on arsenic removal by ferric chloride, *Wat. Res.* 34 (2000) 1255-1261.

[153] M.A. Simeoni, B.D. Batts, C. McRae, Effect of groundwater fulvic acid on the adsorption of arsenate by ferrihydrite and gibbsite, *Appl. Geochem.* 18 (2003) 1507-1515.

[154] S. Goldberg, C.T. Johnston, Mechanism of arsenic adsorption on amorphous oxides evaluated using macroscopic measurements, vibrational spectroscopy, and surface complexation modeling, *J. Colloid Interface Sci.* 234 (2001) 204-216.

[155] Y. Arai, E.V. Elzinga, D.L.Sparks, X-ray absorption spectroscopic investigation of arsenite and arsenate adsorption at the aluminium oxide-water interface, *J. Colloid Interface Sci.* 235 (2001) 80-88.

[156] S. C. B. Myneni, S. J. Traina, G. A. Waychunas, T. J. Logan, Experimental and theoretical vibrational spectroscopic evaluation of arsenate coordination in aqueous solutions, solids, and at mineral-water interfaces, *Geochim. Cosmochim. Acta 62* (1998) 3285-3300.

[157] M. Pena, X. Meng, G.P. Korfiatis, C. Jing, Adsorption mechanism of arsenic on nano-crystalline titanium dioxide, *Environ. Sci. Technol.* 40 (2006) 1257-1262.

[158] A.J. Roddick-Lanzilotta, A. J. McQuillan, D. Craw, Infrared spectroscopic characterization of arsenate (V) ion adsorption from mine waters, Macraes mine, New Zealand, *Appl. Geochem.* 17 (2002) 445-454.

[159] X.-H. Guan, J. Wang, CC. Chusuei, Removal of arsenic from water using granular ferric hydroxide: macroscopic and microscopic studies, *J. Hazard. Mat.* 156 (2008) 178-185.

[160] G. Morin, G. Ona-Nguema, Y. Wang, N. Menguy, F. Juillot, O. Proux, F. Guyot, G. Calas, G. E. Brown Jr., Extended X-ray absorption fine structure analysis of arsenite and arsenate adsorption on maghemite, *Environ. Sci. Technol.* 42 (2008) 2361-2366.

Aalto-DD 37/2013

ISBN 978-952-60-5044-7
ISBN 978-952-60-5045-4 (pdf)
ISSN-L 1799-4934
ISSN 1799-4934
ISSN 1799-4942 (pdf)

Aalto University
School of Engineering
Department of Civil and Environmental Engineering
www.aalto.fi

BUSINESS +
ECONOMY

ART +
DESIGN +
ARCHITECTURE

SCIENCE +
TECHNOLOGY

CROSSOVER

DOCTORAL
DISSERTATIONS